

Resonance model study of kaon production in baryon baryon reactions for heavy ion collisions

K. Tsushima¹ ^{*}, A. Sibirtsev² [†], A. W. Thomas¹ [‡], G. Q. Li³ [§]

¹Department of Physics and Mathematical Physics

and Special Research Center for the Subatomic Structure of Matter

University of Adelaide, SA 5005, Australia

²Institut für Theoretische Physik, Universität Giessen

D-35392 Giessen, Germany

³Department of Physics and Astronomy, State University of New York at Stony Brook

Stony Brook, New York 11794, USA

Abstract

The energy dependence of the total kaon production cross sections in baryon baryon (N and Δ) collisions are studied in the resonance model, which is a relativistic, tree-level treatment. This study is the first attempt to complete a systematic, consistent investigation of the elementary kaon production reactions for both the pion baryon and baryon baryon reactions. Our model suggests that the magnitudes of the isospin-averaged total cross sections for the $NN \rightarrow NYK$ and $\Delta N \rightarrow NYK$ ($Y = \Lambda$ or Σ) reactions are almost equal at energies up to about 200 MeV above threshold. However, the magnitudes for the ΔN reactions become about 6 times larger than those for the NN reactions at energies about 1 GeV above threshold. Furthermore, the magnitudes of the isospin-averaged total cross sections for the $NN \rightarrow \Delta YK$ reactions turn out to be comparable to those for the $NN \rightarrow NYK$ reactions at NN invariant collision energies about 3.1 GeV, and about 5 to 10 times larger at NN invariant collision energies about 3.5 GeV. The microscopic cross sections are parametrized in all isospin channels necessary for the transport model studies of kaon production in heavy ion collisions. These cross sections are then applied in the relativistic transport model to study the sensitivity to the underlying elementary kaon production cross sections.

PACS: 24.10.Jv, 25.40.-h, 25.60.Dz, 25.70.-z, 25.70.Ef, 25.75.Dw

Keywords: Kaon production, Elementary cross sections, Heavy ion collisions, Baryon resonance, One boson exchange, Parametrization

^{*}ktsushim@physics.adelaide.edu.au

[†]sibirt@theorie.physik.uni-giessen.de and on leave from the Institute of Theoretical and Experimental Physics, 117259 Moscow, Russia

[‡]athomas@physics.adelaide.edu.au

[§]gqli@nuclear.physics.sunysb.edu

1 Introduction

Particle production in heavy ion collisions is a unique tool for studying the properties of matter under extreme conditions such as high temperature and/or density [1]-[4]. In particular, positive kaon, K^+ , production in heavy ion collisions at intermediate energies is one of the most promising methods to probe matter formed under such conditions in the central zone of the collisions [5, 6].

Because K^+ -mesons have a long mean free path due to the small cross sections for scattering on nucleons, they can provide us almost undisturbed information about the central zone of heavy ion collisions, in which most of the K^+ -mesons are considered to be produced in sub-threshold heavy ion reactions. According to the theoretical investigations in Refs. [7]-[11], the kaon yield is also very sensitive to the nuclear equation of state. Furthermore, kaon production in heavy ion collisions may provide clues concerning quark gluon plasma formation from the K/π production ratio [12, 13], chiral symmetry restoration [14, 15, 16], and the existence of density isomers [17]. Thus, many studies of kaon production in heavy ion collisions have been made experimentally and theoretically [18]-[62].

The emphasis and focus of earlier theoretical studies was on the momentum-dependent nuclear interactions [20, 21, 22], effects of the rescattering and kaon mass renormalization [23], effects of chiral symmetry restoration [14], and the medium modification of elementary kaon production cross sections [24, 25]. However, most of these theoretical investigations were performed using the energy dependence of the total kaon production cross sections parametrized in a simple phenomenological way [8, 26, 27]. As a consequence, all these investigations involve a certain amount of ambiguity arising from such parametrizations. Furthermore, although recent investigations of strangeness production emphasize the importance of elementary processes such as the $B_1 B_2 \rightarrow B_3 YK$ and $\pi B \rightarrow YK$ reactions [19, 33], no investigations for these reactions have been performed in a consistent manner even in a tree-level treatment. (Here $B_{1,2,3}$ and B stand for either the nucleon or the Δ , while Y stands for either the Λ or the Σ hyperon.)

Although many issues need to be considered in order to achieve a better understanding of kaon production in heavy ion collisions, the one emphasized in this article is the elementary kaon production cross sections at the hadronic level as was studied in Refs. [28, 29, 30, 31, 38, 42, 44, 46]. Since most of the microscopic transport models assume that the relevant reactions are described by on-shell, binary interactions at the hadronic level, it should be straightforward to improve the parametrizations for the elementary kaon production cross sections, which are important inputs of the models.

Recently, the COSY-11 Collaboration [34] measured the total cross section for the $pp \rightarrow p\Lambda K^+$ reaction at an energy 2 MeV above the reaction threshold. The result distinctly differs from those of the commonly used phenomenological parametrizations [8, 26]. However, in practice, this discrepancy probably does not significantly influence the past results calculated using the parametrizations made without this new data point, because the magnitudes of the cross sections at this energy are very small for both the experiment [34] and parametrizations [8, 26].

On the other hand, theoretical reanalyses in Refs. [35, 36, 37] using different parametrizations [38] for the $NN \rightarrow NYK$ cross sections, indicate that the secondary reactions, $\pi N \rightarrow YK$, give rather important contributions – comparable with those of the baryon baryon (N and Δ) induced reactions. This conclusion contradicts the previously accepted scenario, in which the dominant contributions for K^+ production in heavy ion collisions come from ΔN and $\Delta\Delta$ collisions [10, 39, 40, 41, 42]. Thus, it is necessary to investigate further the elementary kaon

production cross sections for both the $\pi B \rightarrow YK$ and $B_1 B_2 \rightarrow B_3 YK$ reactions in a consistent manner. Furthermore, all the conclusions drawn about the elementary reactions involving a Δ were based on the results obtained using the elementary cross sections for the nucleon, not for the Δ , except for the isospin difference. Thus, an explicit calculation for the cross sections involving a Δ should be performed, treating properly not only isospin degrees of freedom but also spin as was initially attempted in Ref. [42] using the results of the resonance model for the $\pi B \rightarrow YK$ reactions [46].

For this purpose, we complete our systematic investigations for the elementary kaon production processes in all baryon baryon reactions, extending the studies made so far for the pion baryon and proton proton reactions using the resonance model [44, 45]. The treatment of the present study is a tree-level, using empirical branching ratios for the relevant resonances. It is relativistic, and incorporates the pion baryon, and the baryon baryon reactions in a consistent manner. Thus, most of the cut-off parameters, coupling constants and form factors have been fixed already in pion baryon and proton proton reactions [44, 46]. Furthermore, we parametrize the energy dependence of these total kaon production cross sections in baryon baryon collisions for all the isospin channels needed in the simulation codes. We note that the total cross sections for the $pp \rightarrow p\Lambda K^+$ reaction recently measured at energies about 50 and 150 MeV above threshold [47] show an excellent agreement with the predicted results of the resonance model [44]. However, because the treatment in the model does not include the final state interactions, our results cannot be expected to describe well the near-threshold behaviour. A more rigorous treatment of the resonances consistent with the unitary condition was studied by Fuester and Mosel [43], but such an approach does not seem to be suitable for the present purpose, and beyond the scope of the present study.

The organization of this article is as follows. In Sect. 2 we will explain the resonance model in detail. Effective Lagrangian densities at the hadronic level together with the experimental data for the model will be described. Numerical results for the total cross sections will be presented in Sec. 3. In Sect. 4 we give all the parametrizations for the energy dependence of the total cross sections calculated in the model. In Sec. 5 these cross sections are used in the relativistic transport model to study the sensitivity of the transport model predictions to the underlying elementary kaon production cross sections. Discussions and summary will be given in Sect. 6. Finally, in the Appendix, the relations between the branching ratios of the resonances and the coupling constants relevant for the model will be given. In addition, we will supplement the cross section relations for the $\pi N \rightarrow \Lambda K$ reaction which were not mentioned in Ref. [46].

2 Resonance model

In Fig. 1, we show the Feynman diagrams relevant for kaon production in the resonance model. R stands for the baryon resonances which are responsible for the kaon and hyperon pair production, with their masses up to about 2 GeV. Assumptions and approximations of the model are [44, 45, 46]:

1. Resonances which are experimentally observed to decay to hyperon and kaon are included in the model. A kaon is always produced from these resonances simultaneously with a hyperon. In the study of the $\pi B \rightarrow YK$ reactions, we have also investigated the non-resonant contributions, including an effective t -channel K^* -meson exchange. It turned out that this non-resonant contribution was small in order to reproduce the experimental

data, once the relevant s -channel resonances were included in the model [46]. Thus, kaon exchange which is included in Refs. [28, 30, 31, 38, 42] and would introduce extra new parameters in the present treatment, is not included in the present calculation. Instead, other meson exchanges, namely η and ρ meson exchanges, are included, and they compensate the contribution of kaon exchange introduced in other models.

2. Mesons exchanged are restricted to those observed in the decay channels of the adopted resonances. (See also Fig. 1.) We note that there is a discussion in Ref. [45] of whether there is a possibility to settle what kind of meson exchange is responsible for the $pp \rightarrow p\Lambda K^+$ reaction.
3. Those processes in which the exchanged pion can be on-shell are excluded, because on-shell pions are usually included as secondary processes in microscopic transport models through processes such as $\pi N \leftrightarrow \Delta$ and $\pi B \rightarrow YK$. Thus, the $\Delta\Delta \rightarrow NYK$ reactions, which are possible only through π -exchange in the model, are not included. Note that because of the assumption made in number 2, neither ρ -meson nor η -meson exchanges will give contributions to this channel in the present treatment.
4. Resonances are treated as elementary particles, except that their observed widths enter in the propagators. Because of this, ρ -exchange attached to the $N(1650)$ resonance is excluded kinematically, although this resonance has a branch in the $N\rho$ channel [63].
5. Any final state interactions which are usually important for describing the near-threshold behaviour are not included. Thus, our results should not be taken seriously near the reaction threshold, which is different from the present main purpose.

It is worth noting that all values of the coupling constants squared relevant for the meson-baryon-(baryon resonance) vertices, g_{MBR}^2 ($M = \pi, \eta, \rho$), can be determined from the experimental decay ratios, once the interaction Lagrangian densities and relevant form factors are specified. In Table 1 we summarize the data for those resonances which are included in the model, and necessary to calculate the coupling constants.

Effective Lagrangian densities relevant for evaluating the Feynman diagrams depicted in Fig. 1 are:

$$\mathcal{L}_{\pi NN} = -ig_{\pi NN}\bar{N}\gamma_5\vec{\tau}N \cdot \vec{\pi}, \quad (1)$$

$$\mathcal{L}_{\pi N\Delta} = -\frac{g_{\pi N\Delta}}{m_\pi} \left(\bar{\Delta}^\mu \vec{\mathcal{I}} N \cdot \partial_\mu \vec{\pi} + \bar{N} \vec{\mathcal{I}}^\dagger \Delta^\mu \cdot \partial_\mu \vec{\pi} \right), \quad (2)$$

$$\mathcal{L}_{\pi NN(1650)} = -g_{\pi NN(1650)} \left(\bar{N}(1650)\vec{\tau}N \cdot \vec{\pi} + \bar{N}\vec{\tau}N(1650) \cdot \vec{\pi} \right), \quad (3)$$

$$\mathcal{L}_{\pi NN(1710)} = -ig_{\pi NN(1710)} \left(\bar{N}(1710)\gamma_5\vec{\tau}N \cdot \vec{\pi} + \bar{N}\gamma_5\vec{\tau}N(1710) \cdot \vec{\pi} \right), \quad (4)$$

$$\mathcal{L}_{\pi NN(1720)} = \frac{g_{\pi NN(1720)}}{m_\pi} \left(\bar{N}^\mu(1720)\vec{\tau}N \cdot \partial_\mu \vec{\pi} + \bar{N}\vec{\tau}N^\mu(1720) \cdot \partial_\mu \vec{\pi} \right), \quad (5)$$

$$\mathcal{L}_{\pi N\Delta(1920)} = \frac{g_{\pi N\Delta(1920)}}{m_\pi} \left(\bar{\Delta}^\mu(1920)\vec{\mathcal{I}} N \cdot \partial_\mu \vec{\pi} + \bar{N} \vec{\mathcal{I}}^\dagger \Delta^\mu(1920) \cdot \partial_\mu \vec{\pi} \right), \quad (6)$$

$$\mathcal{L}_{\pi\Delta\Delta} = -ig_{\pi\Delta\Delta}\bar{\Delta}_\mu\gamma_5\vec{\mathcal{K}}\Delta^\mu \cdot \vec{\pi}, \quad (7)$$

$$\mathcal{L}_{\pi\Delta N(1650)} = i\frac{g_{\pi\Delta N(1650)}}{m_\pi} \left(\bar{N}(1650)\gamma_5\vec{\mathcal{I}}^\dagger \Delta^\mu \cdot \partial_\mu \vec{\pi} + \bar{\Delta}^\mu\gamma_5\vec{\mathcal{I}} N(1650) \cdot \partial_\mu \vec{\pi} \right), \quad (8)$$

$$\mathcal{L}_{\pi\Delta N(1710)} = \frac{g_{\pi\Delta N(1710)}}{m_\pi} \left(\bar{N}(1710)\vec{\mathcal{I}}^\dagger \Delta^\mu \cdot \partial_\mu \vec{\pi} + \bar{\Delta}\vec{\mathcal{I}} N(1710) \cdot \partial_\mu \vec{\pi} \right), \quad (9)$$

Table 1: Resonances included in the model. Confidence levels of the resonances are, $N(1650) * ***$, $N(1710) * **$, $N(1720) * ***$ and $\Delta(1920) * **$ [63]. Note that the $\Delta(1920)$ resonance is treated as an effective resonance which represents all contributions of six resonances, $\Delta(1900)$, $\Delta(1905)$, $\Delta(1910)$, $\Delta(1920)$, $\Delta(1930)$ and $\Delta(1940)$. See Ref. [46] for this effective treatment of the $\Delta(1920)$.

Resonance (J^P)	Width (MeV)	Decay channel	Branching ratio	Adopted value
$N(1650) (\frac{1}{2}^-)$	150	$N\pi$	0.60 – 0.80	0.700
		$N\eta$	0.03 – 0.10	0.065
		$\Delta\pi$	0.03 – 0.07	0.050
		ΛK	0.03 – 0.11	0.070
$N(1710) (\frac{1}{2}^+)$	100	$N\pi$	0.10 – 0.20	0.150
		$N\eta$	0.20 – 0.40	0.300
		$N\rho$	0.05 – 0.25	0.150
		$\Delta\pi$	0.10 – 0.25	0.175
		ΛK	0.05 – 0.25	0.150
		ΣK	0.02 – 0.10	0.060
$N(1720) (\frac{3}{2}^+)$	150	$N\pi$	0.10 – 0.20	0.150
		$N\eta$	0.02 – 0.06	0.040
		$N\rho$	0.70 – 0.85	0.775
		$\Delta\pi$	0.05 – 0.15	0.100
		ΛK	0.03 – 0.10	0.065
		ΣK	0.02 – 0.05	0.035
$\Delta(1920) (\frac{3}{2}^+)$	200	$N\pi$	0.05 – 0.20	0.125
		ΣK	0.01 – 0.03	0.020

$$\mathcal{L}_{\pi\Delta N(1720)} = -ig_{\pi\Delta N(1720)} \left(\bar{N}_\mu(1720) \gamma_5 \vec{\mathcal{I}}^\dagger \Delta^\mu \cdot \vec{\pi} + \bar{\Delta}^\mu \gamma_5 \vec{\mathcal{I}} N^\mu(1720) \cdot \vec{\pi} \right), \quad (10)$$

$$\mathcal{L}_{\eta NN} = -ig_{\eta NN} \bar{N} \gamma_5 N \eta, \quad (11)$$

$$\mathcal{L}_{\eta\Delta\Delta} = -ig_{\eta\Delta\Delta} \bar{\Delta}_\mu \gamma_5 \Delta^\mu \eta, \quad (12)$$

$$\mathcal{L}_{\eta NN(1650)} = -g_{\eta NN(1650)} \left(\bar{N}(1650) N \eta + \bar{N} N(1650) \eta \right), \quad (13)$$

$$\mathcal{L}_{\eta NN(1710)} = -ig_{\eta NN(1710)} \left(\bar{N}(1710) \gamma_5 N \eta + \bar{N} \gamma_5 N(1710) \eta \right), \quad (14)$$

$$\mathcal{L}_{\eta NN(1720)} = \frac{g_{\eta NN(1720)}}{m_\eta} \left(\bar{N}^\mu(1720) N \partial_\mu \eta + \bar{N} N^\mu(1720) \partial_\mu \eta \right), \quad (15)$$

$$\mathcal{L}_{\rho NN} = -g_{\rho NN} \left(\bar{N} \gamma^\mu \vec{\tau} N \cdot \vec{\rho}_\mu + \frac{\kappa}{2m_N} \bar{N} \sigma^{\mu\nu} \vec{\tau} N \cdot \partial_\mu \vec{\rho}_\nu \right), \quad (16)$$

$$\mathcal{L}_{\rho\Delta\Delta} = g_{\rho\Delta\Delta} \bar{\Delta}_\mu \gamma^\nu \vec{\mathcal{K}} \Delta^\mu \cdot \vec{\rho}_\nu, \quad (17)$$

$$\mathcal{L}_{\rho N\Delta} = -i \frac{g_{\rho N\Delta}}{m_\rho} \left(\bar{\Delta}^\mu \gamma^\nu \gamma_5 \vec{\mathcal{I}} N + \bar{N} \gamma^\mu \gamma_5 \vec{\mathcal{I}}^\dagger \Delta^\nu \right) \cdot (\partial_\mu \vec{\rho}_\nu - \partial_\nu \vec{\rho}_\mu), \quad (18)$$

$$\mathcal{L}_{\rho NN(1710)} = -g_{\rho NN(1710)} \left(\bar{N}(1710) \gamma^\mu \vec{\tau} N \cdot \vec{\rho}_\mu + \bar{N} \gamma^\mu \vec{\tau} N(1710) \cdot \vec{\rho}_\mu \right), \quad (19)$$

$$\mathcal{L}_{\rho NN(1720)} = -ig_{\rho NN(1720)} \left(\bar{N}^\mu(1720) \gamma_5 \vec{\tau} N \cdot \vec{\rho}_\mu + \bar{N} \gamma_5 \vec{\tau} N^\mu(1720) \cdot \vec{\rho}_\mu \right), \quad (20)$$

$$\mathcal{L}_{K\Lambda N(1650)} = -g_{K\Lambda N(1650)} \left(\bar{N}(1650) \Lambda K + \bar{K} \bar{\Lambda} N(1650) \right), \quad (21)$$

$$\mathcal{L}_{K\Sigma N(1710)} = -ig_{K\Lambda N(1710)} \left(\bar{N}(1710) \gamma_5 \Lambda K + \bar{K} \bar{\Lambda} \gamma_5 N(1710) \right), \quad (22)$$

$$\mathcal{L}_{K\Lambda N(1720)} = \frac{g_{K\Lambda N(1720)}}{m_K} \left(\bar{N}^\mu(1720) \Lambda \partial_\mu K + (\partial_\mu \bar{K}) \bar{\Lambda} N^\mu(1720) \right), \quad (23)$$

$$\mathcal{L}_{K\Sigma N(1710)} = -ig_{K\Sigma N(1710)} \left(\bar{N}(1710) \gamma_5 \vec{\tau} \cdot \vec{\Sigma} K + \bar{K} \vec{\Sigma} \cdot \vec{\tau} \gamma_5 N(1710) \right), \quad (24)$$

$$\mathcal{L}_{K\Sigma N(1720)} = \frac{g_{K\Sigma N(1720)}}{m_K} \left(\bar{N}^\mu(1720) \vec{\tau} \cdot \vec{\Sigma} \partial_\mu K + (\partial_\mu \bar{K}) \vec{\Sigma} \cdot \vec{\tau} N^\mu(1720) \right), \quad (25)$$

$$\mathcal{L}_{K\Sigma\Delta(1920)} = \frac{g_{K\Sigma\Delta(1920)}}{m_K} \left(\bar{\Delta}^\mu(1920) \vec{\mathcal{I}} \cdot \vec{\Sigma} \partial_\mu K + (\partial_\mu \bar{K}) \vec{\Sigma} \cdot \vec{\mathcal{I}}^\dagger \Delta^\mu(1920) \right). \quad (26)$$

In the above, the operators $\vec{\mathcal{I}}$ and $\vec{\mathcal{K}}$ are defined by

$$\vec{\mathcal{I}}_{M\mu} \equiv \sum_{\ell=\pm 1,0} (1\ell \frac{1}{2}\mu | \frac{3}{2}M) \hat{e}_\ell^*, \quad (27)$$

$$\vec{\mathcal{K}}_{MM'} \equiv \sum_{\ell=\pm 1,0} (1\ell \frac{3}{2}M' | \frac{3}{2}M) \hat{e}_\ell^*, \quad (28)$$

with M , μ and M' being the third components of the isospin projections, and $\vec{\tau}$ the Pauli matrices. $N, N(1710), N(1720)$ and $\Delta(1920)$ stand for the fields of the nucleon and the corresponding baryon resonances. They are expressed by $\bar{N} = (\bar{p}, \bar{n})$, similarly for the nucleon resonances, and $\bar{\Delta}(1920) = (\bar{\Delta}(1920)^{++}, \bar{\Delta}(1920)^+, \bar{\Delta}(1920)^0, \bar{\Delta}(1920)^-)$ in isospin space. The physical representations of the kaon field are, $K^T = (K^+, K^0)$ and $\bar{K} = (K^-, \bar{K}^0)$, respectively, where the superscript T means the transposition operation. They are defined as annihilating (creating) the physical particle (anti-particle) states. For the propagators $iS_F(p)$ of the spin 1/2 and $iG^{\mu\nu}(p)$ of the spin 3/2 resonances we use:

$$iS_F(p) = i \frac{\gamma \cdot p + m}{p^2 - m^2 + im\Gamma_{full}}, \quad (29)$$

$$iG^{\mu\nu}(p) = i \frac{-P^{\mu\nu}(p)}{p^2 - m^2 + im\Gamma^{full}}, \quad (30)$$

with

$$P^{\mu\nu}(p) = -(\gamma \cdot p + m) \left[g^{\mu\nu} - \frac{1}{3}\gamma^\mu\gamma^\nu - \frac{1}{3m}(\gamma^\mu p^\nu - \gamma^\nu p^\mu) - \frac{2}{3m^2}p^\mu p^\nu \right], \quad (31)$$

where m and Γ^{full} stand for the mass and full decay width of the corresponding resonances. For the form factors, $F_M(\vec{q})$ (\vec{q} is the momentum of meson, M), appearing in the meson-baryon-baryon resonance vertices, we use

$$F_M(\vec{q}) = \left(\frac{\Lambda_M^2}{\Lambda_M^2 + \vec{q}^2} \right)^n, \quad (32)$$

where $n = 1$ for the π and η -mesons and $n = 2$ for the ρ -meson, respectively, with Λ_M being the cut-off parameter. Most of the form factors, coupling constants and cut-off parameters for the relevant meson-baryon-baryon and meson-baryon-(baryon resonance) vertices are adopted from Refs. [44, 46]. In the Appendix, we give the relations between the branching ratios and the corresponding coupling constants squared, g_{MBR}^2 , which were calculated using the relevant Lagrangian densities. In the calculation, the form factors of Eq. (32) are multiplied by the corresponding coupling constants, g_{MBR} . For the coupling constants, $g_{M\Delta\Delta}$ ($M = \pi, \eta, \rho$), which appeared for the first time in the present study, we use an SU(6) quark model result with the definition Eq. (28), $g_{M\Delta\Delta} = 3g_{MNN}$. In addition, we use the same value for the corresponding cut-off parameter as that for the nucleon. For the value of the cut-off parameter at the $\rho N\Delta$ vertex, we use $544 = 1300 \times (920/2200)$ MeV, which is scaled the same amount as was necessary for the ρNN vertex of the Bonn potential model (the Model I in Table B.1 [64]). The other quantities, coupling constants, cut-off parameters and form factors are, as far as possible, taken from the same version of the model [64]. In addition, we use a value, $\kappa = f_{\rho NN}/g_{\rho NN} = 6.1$, for the tensor coupling constant at the ρNN vertex. We summarize in Table 2 all values for the coupling constants and cut-off parameters used in the study.

3 Numerical results

In this study, we neglected all interference terms between the amplitudes. Thus, the relations given in this section for the cross sections are not always valid when the interference terms are included rigorously.

3.1 $NN \rightarrow NYK$

Recently, the total cross section for the $pp \rightarrow p\Lambda K^+$ reaction was measured by the COSY 11 Collaboration [34] at energies of a few MeV above the reaction threshold, and it gave a new constraint on the theoretical calculations and phenomenological parametrizations. However, we do not refit the parameters and coupling constants to this new data point for the following reasons. First, our treatment does not include the final state interactions nor interference terms, which will be important at energies very near threshold. Second, the total cross sections at energies up to about 10 MeV above the threshold are very small in magnitude for both the parametrization and the new data point. Thus, this new data point will not influence the calculation of kaon yield in heavy ion collisions (for instance see Fig. 9 in Ref. [35]).

Table 2: Coupling constants and cut-off parameters used in the present study. $\kappa = f_{\rho NN}/g_{\rho NN} = 6.1$ is used for the ρNN tensor coupling. Note that the coupling constants relevant for $\Delta(1920)$, $g_{\pi N\Delta(1920)}$ and $g_{K\Sigma\Delta(1920)}$, are scaled multiplying by a factor 1.86 according to the effective treatment [46]. See also the caption of Table 1.

vertex	$g^2/4\pi$	cut-off (MeV)	vertex	$g^2/4\pi$	cut-off (MeV)
πNN	14.4	1050	$\pi\Delta\Delta$	$3^2 \times 14.4$	1050
$\pi NN(1650)$	1.12×10^{-1}	800	$\pi NN(1710)$	2.05×10^{-1}	800
$\pi NN(1720)$	4.13×10^{-3}	800	$\pi N\Delta(1920)$	1.13×10^{-1}	500
$\pi\Delta N(1650)$	7.19×10^{-2}	800	$\pi\Delta N(1710)$	2.23×10^{-3}	800
$\pi\Delta N(1720)$	1.39	800	ηNN	5.00	2000
$\eta\Delta\Delta$	$3^2 \times 5.00$	2000	$\eta NN(1650)$	3.37×10^{-2}	800
$\eta NN(1710)$	2.31	800	$\eta NN(1720)$	1.03×10^{-1}	800
ρNN	0.74	920	$\rho N\Delta$	19.0	544
$\rho\Delta\Delta$	$3^2 \times 0.74$	920	$\rho NN(1710)$	$3.61 \times 10^{+1}$	800
$\rho NN(1720)$	$1.43 \times 10^{+2}$	800	$K\Lambda N(1650)$	5.10×10^{-2}	800
$K\Lambda N(1710)$	3.78	800	$K\Lambda N(1720)$	3.12×10^{-1}	800
$K\Sigma N(1710)$	4.66	800	$K\Sigma N(1720)$	2.99×10^{-1}	800
$K\Sigma\Delta(1920)$	3.08×10^{-1}	500			

Here, we write down explicitly the amplitude and cross section formula for the $pp \rightarrow p\Lambda K^+$ reaction, as an example. The total amplitude for this reaction is given by

$$\begin{aligned} \mathcal{M} = & \mathcal{M}(p(1650), \pi^0) + \mathcal{M}(p(1710), \pi^0) + \mathcal{M}(p(1720), \pi^0) \\ & + \mathcal{M}(p(1650), \eta) + \mathcal{M}(p(1710), \eta) + \mathcal{M}(p(1720), \eta) \\ & + \mathcal{M}(p(1710), \rho^0) + \mathcal{M}(p(1720), \rho^0) + (\text{exchange terms}), \end{aligned} \quad (33)$$

where on the right hand side of Eq. (33), the resonances and mesons exchanged in the intermediate states are written inside the bracket explicitly. Each amplitude can be obtained straightforwardly by applying the Feynman rules with the relevant interaction Lagrangian densities.

For a given invariant collision energy, \sqrt{s} , the total cross section, $\sigma(pp \rightarrow p\Lambda K^+)$, can be calculated by

$$\sigma(pp \rightarrow p\Lambda K^+) = \frac{1}{F} \int |\overline{\mathcal{M}}|^2 \delta^4(p_1 + p_2 - p_3 - p_\Lambda - p_K) \frac{d^3 p_3}{2E_3} \frac{d^3 p_\Lambda}{2E_\Lambda} \frac{d^3 p_K}{2E_K}, \quad (34)$$

with the flux factor

$$\begin{aligned} F = & 2 \lambda^{1/2}(s, m_p^2, m_p^2) (2\pi)^5, \\ \lambda(x, y, z) \equiv & x^2 + y^2 + z^2 - xy - yz - zx, \end{aligned}$$

where the subscripts 1 and 2 stand for the initial protons, and 3 for the final proton, corresponding to the diagrams in Fig. 1 for $\sigma(B_1 B_2 \rightarrow B_3 Y K)$. This notation, corresponding to

Fig. 1, will be used hereafter. $|\bar{\mathcal{M}}|^2$ is the square of the scattering amplitude, averaged over the initial spins and summed over the final spins. To perform the integration over the final state three-body phase space, we first integrate on $d^3 p_3$ and $d^3 p_\Lambda$ in the center-of-mass (c.m.) frame of the final state proton and Λ , and then integrate on $d^3 p_K$ in the c.m. frame of the initial protons [65] using the Lorentz transformation. Note that our treatment neglects all interference terms and final state interactions [51, 52] which are important in near-threshold energy region. For the effect of the interference terms in the model, one can find a discussion in Ref. [44].

Fig. 2 illustrates the separate contributions from π , ρ and η -exchanges to the total cross sections for the $pp \rightarrow p\Lambda K^+$ reaction. \sqrt{s} is the pp invariant collision energy in their c.m. system, while $\sqrt{s_0} = m_N + m_\Lambda + m_K$ is the threshold energy with m_N , m_Λ and m_K being respectively the masses of the nucleon, Λ and kaon. One can see that pion exchange is dominant at energies near the reaction threshold, while ρ -exchange is dominant at higher energies.

As was already discussed in Ref. [44], the total cross section is rather sensitive to the value of the cut-off parameter, Λ_ρ , in the ρNN vertex form factor at higher energies. The dependence on the values of the cut-off parameter, Λ_ρ , and coupling constant, $g_{\rho NN}$, is shown in Fig. 3. After fixing the cut-off parameter to a specific value, the sensitivity of the total cross section to the ρNN coupling constant, $g_{\rho NN}$, (with $\kappa = 6.1$ for the tensor coupling constant) is small. The best values to reproduce the experimental data [49] at energies larger than about 100 MeV above threshold were found to be, $g_{\rho NN}^2/4\pi = 0.74$ and $\Lambda_\rho = 920$ MeV.

Since the total cross sections for the reaction at energies just above threshold receive their dominant contribution from pion exchange, we will test the sensitivity of the results to the value of the cut-off parameter in the πNN form factor, $\Lambda_{\pi NN}$. Although the cut-off and coupling constant, $g_{\pi NN}$ and $\Lambda_{\pi NN}$, are not independent in a strict sense, when they are determined from the NN phase shift data, we will show the results calculated using two different values for the cut-off parameter, $\Lambda_{\pi NN} = 3000$ MeV and 1050 MeV, with the fixed, usually accepted value, $g_{\pi NN}^2/4\pi = 14.4$. The adopted value from this reaction for the cut-off parameter is, $\Lambda_{\pi NN} = 1050$ MeV.

In Fig. 4 we show the total cross sections for the $pp \rightarrow p\Lambda K^+$ reaction calculated with the two different cut-offs, $\Lambda_{\pi NN} = 3000$ MeV (the solid line) and $\Lambda_{\pi NN} = 1050$ MeV (the dashed line), together with the experimental data [34, 49]. Results are rather insensitive to the value, $\Lambda_{\pi NN}$. The new data point from COSY [34] does not seem to be achieved by varying the value of the $\Lambda_{\pi NN}$ within a reasonable range. However, it is worth noting that the parameter set fixed by the $pp \rightarrow p\Lambda K^+$ reaction, including the cut-off $\Lambda_{\pi NN}$, must be used also for the calculation of the $NN \rightarrow N\Sigma K$ reactions. It is not trivial at all if the same parameter set could also reproduce the experimental data for the $NN \rightarrow N\Sigma K$ reactions. Furthermore, although the parameters were optimised so as to reproduce the data points around 1 GeV above threshold, the recent data for the total cross sections measured at energies about 50 and 150 MeV above the threshold [47] show an excellent agreement with the predicted values of the resonance model [44]. This provides some confirmation of the validity of the parameters determined in the model.

Next, we will discuss the $pp \rightarrow N\Sigma K$ reactions. In Fig. 5 we show the separate contributions from π , ρ and η -exchange to the total cross sections for the $pp \rightarrow p\Sigma^0 K^+$ reaction. The ρ -exchange is again dominant at higher energies, while the η and π -exchanges are dominant near the threshold. The larger contribution from the η -exchange compared to that of π -exchange, which contrasts with the $pp \rightarrow p\Lambda K^+$ reaction, is due to the large $\eta NN(1710)$ coupling constant, i.e., the large branching ratio of the $N(1710)$ resonance to the ηN channel. (See also Tables 1 and 2.)

The energy dependence of the total cross sections for the $pp \rightarrow p\Sigma^+K^0$, $pp \rightarrow p\Sigma^0K^+$ and $pp \rightarrow n\Sigma^+K^+$ reactions is shown in Fig. 6, together with the experimental data [49]. The threshold is, $\sqrt{s_0} = m_N + m_\Sigma + m_K$, with m_Σ the mass of the Σ -hyperon. The solid and dashed lines indicate the results calculated using the two different values the cut-off parameter, $\Lambda_{\pi NN} = 3000$ MeV and 1050 MeV, respectively. Although the deviations of the experimental data are relatively large, our model with the adopted cut-off parameter value, $\Lambda_{\pi NN} = 1050$ MeV, reproduces the data fairly well using the values, $g_{\rho NN}^2/4\pi = 0.74$ and $\Lambda_\rho = 920$ MeV, fixed in the $pp \rightarrow p\Lambda K^+$ reaction.

In Fig. 7, we show energy dependence of the total cross sections for the $pn \rightarrow p\Lambda K^0$, $np \rightarrow p\Sigma^0K^0$ and $np \rightarrow p\Sigma^-K^+$ reactions together with the experimental data [49]. The results are again shown for the two values of $\Lambda_{\pi NN}$, where the results calculated with the value, $\Lambda_{\pi NN} = 1050$ MeV (the dashed lines in Fig. 7) should be compared with the data. At energies about 1 GeV above the threshold, the magnitudes of the total cross sections calculated using the two different values of the cut-off, $\Lambda_{\pi NN}$, become almost equal. This is because, at these energies, the momentum of the exchanged pion becomes large and the πNN form factor [64] is insensitive to the value of the cut-off parameter, $\Lambda_{\pi NN}$. The model results (the dashed lines) overestimate the experimental data roughly a factor 2, or at most a factor of 7 for one data point, although the same parameter set reproduces the data for the $pp \rightarrow p\Lambda K^+$ reaction fairly well. However, the overestimate of about a factor 2 for the $pn \rightarrow p\Lambda K^0$ reaction, can be contrasted with the finding of Fäldt and Wilkin [51], that the results for the reaction with a neutron target differs by factors of 5 to 10. Their calculation included the $N(1650)$ resonance alone with pion exchange, which is included as one of the contributions in the present calculation.

We should comment about the discrepancies between the calculated results and the neutron data. Our calculations for the $pn(np) \rightarrow NYK$ reactions are based on SU(2) symmetry which should be very good for the present purpose. For the given Lagrangian densities, which are explained in Sec. 2, the calculations for the $pn(np) \rightarrow NYK$ reactions are trivially related to the $pp \rightarrow NYK$ reactions through isospin symmetry. We do not have any new mechanism to introduce in the model in calculating the $pn(np) \rightarrow NYK$ reactions – except for charge symmetry breaking, which cannot be expected to lead to such a huge difference between the $pn(np) \rightarrow NYK$ and $pp \rightarrow NYK$ reactions. We should also comment that the data for the $pn(np) \rightarrow NYK$ reactions tabulated in Ref. [49] are taken from Ref. [50], whose data contain a systematic uncertainty of $\sim 13\%$ in the neutron beam normalization, where that error is not included in Fig. 7. Furthermore, their analysis [50] was based on a number of hypotheses, which in principle, could be strongly model dependent. Thus, we would like to emphasize that it is necessary to investigate further the reactions involving a neutron in the initial state, both theoretically and experimentally.

The total cross sections for the K^0 production channels are obtained by

$$\sigma(pp \rightarrow p\Lambda K^+) = \sigma(nn \rightarrow n\Lambda K^0), \quad (35)$$

$$\sigma(pn \rightarrow n\Lambda K^+) = \sigma(np \rightarrow p\Lambda K^0), \quad (36)$$

$$\sigma(pp \rightarrow p\Sigma^0K^+) = \sigma(nn \rightarrow n\Sigma^0K^0), \quad (37)$$

$$\sigma(pp \rightarrow n\Sigma^+K^+) = \sigma(nn \rightarrow n\Sigma^-K^0), \quad (38)$$

$$\sigma(pn \rightarrow n\Sigma^0K^+) = \sigma(np \rightarrow p\Sigma^0K^0), \quad (39)$$

$$\sigma(np \rightarrow p\Sigma^-K^+) = \sigma(pn \rightarrow n\Sigma^+K^0), \quad (40)$$

$$\sigma(nn \rightarrow n\Sigma^-K^+) = \sigma(pp \rightarrow p\Sigma^+K^0). \quad (41)$$

3.2 $NN \rightarrow \Delta YK$

One expects that contributions from the $NN \rightarrow \Delta YK$ reactions to the kaon yield in heavy ion collisions are small, because of the high threshold energy. Thus, usually these reactions are not included in simulation codes. However, there has been no explicit theoretical estimate for the reactions.

In Fig. 8 we show the energy dependence of the total cross sections for the $nn \rightarrow \Delta^- \Lambda K^+$ and $pp \rightarrow \Delta^{++} \Sigma^- K^+$ reactions. At NN invariant collision energies about 3.1 GeV, the magnitudes of the total cross sections for both reactions become about $70 \mu b$. These magnitudes are comparable with that of the $pp \rightarrow p \Lambda K^+$ reaction at these energies. However, they become about 10 times larger than those of the $pp \rightarrow p \Lambda K^+$ reaction at NN invariant collision energies about 3.5 GeV. Thus, these reactions, which are usually discarded in theoretical studies of kaon production in heavy ion collisions, might give large contributions to the kaon yield, if there are plenty of NN pairs which have such collision energies.

In order to make an estimate of the uncertainty in the calculation for these reactions, we make a comparison with the data for the $pp \rightarrow N \pi YK$ reactions in Fig. 9. Note that these reactions have different thresholds, but the comparison should be helpful in judging whether the results contain more than a order of magnitude uncertainties. We restrict ourselves to NN invariant collision energies below about 3.5 GeV (as we do throughout this paper) the predictions are certainly of the same order of magnitude as the data and therefore not unreasonable. We conclude that the $NN \rightarrow \Delta YK$ reactions may be equally as important as the $NN \rightarrow NYK$ reactions for heavy ion simulations. However, this argument should be checked eventually by heavy ion simulations, keeping in mind the theoretical uncertainties.

The total cross sections for the other isospin channels are obtained by

$$\begin{aligned} \sigma(nn \rightarrow \Delta^- \Lambda K^+) &= \sigma(pp \rightarrow \Delta^{++} \Lambda K^0) \\ &= 3\sigma(pn \rightarrow \Delta^0 \Lambda K^+) = 3\sigma(np \rightarrow \Delta^+ \Lambda K^0) \\ &= 3\sigma(pp \rightarrow \Delta^+ \Lambda K^+) = 3\sigma(nn \rightarrow \Delta^0 \Lambda K^0), \end{aligned} \quad (42)$$

$$\begin{aligned} \sigma(pp \rightarrow \Delta^{++} \Sigma^- K^+) &= \sigma(nn \rightarrow \Delta^- \Sigma^+ K^0) \\ &= 2\sigma(nn \rightarrow \Delta^- \Sigma^0 K^+) = 2\sigma(pp \rightarrow \Delta^{++} \Sigma^0 K^0) \\ &= 3\sigma(np \rightarrow \Delta^+ \Sigma^- K^+) = 3\sigma(pp \rightarrow \Delta^+ \Sigma^+ K^0) \\ &= 3\sigma(nn \rightarrow \Delta^0 \Sigma^- K^+) = 3\sigma(pn \rightarrow \Delta^0 \Sigma^+ K^0) \\ &= 6\sigma(pp \rightarrow \Delta^+ \Sigma^0 K^+) = 6\sigma(np \rightarrow \Delta^+ \Sigma^0 K^0) \\ &= 6\sigma(pn \rightarrow \Delta^0 \Sigma^0 K^+) = 6\sigma(nn \rightarrow \Delta^0 \Sigma^0 K^0). \end{aligned} \quad (43)$$

3.3 $\Delta N \rightarrow NYK$

According to the simulation results [10, 39, 40, 41, 42], it is widely believed that kaons are mostly produced through the $\Delta N \rightarrow NYK$ and $\Delta \Delta \rightarrow NYK$ reactions in heavy ion collisions. However, in most of the theoretical studies with the Boltzmann/Vlasov-Uehling-Uhlenbeck approach (BUU/VUU) [1, 53, 54, 55, 56, 57], or quantum molecular dynamics (QMD) [58, 59], the parametrizations used for these total cross sections have been made in a simple phenomenological manner in free space [8, 26, 27]. In addition, the parametrizations for all isospin channels are obtained by fitting to the existing limited isospin channels of the data. Furthermore, those parametrizations for the reactions involving a Δ or Δ 's used to draw the conclusion [10, 39, 40, 41, 33, 60], are obtained using the cross sections for the nucleon except for the

isospin difference [26]. In addition, the coupling constants relevant for the Δ are assumed to be equal to those for the nucleon, e.g., $F_{NN\pi} = F_{N\Delta\pi}$ and $F_{\Delta\Delta\pi} = F_{NN\pi}$.

Recently, this isospin symmetry ansatz suggested in Ref. [26] has been reconsidered Li and Ko [42], and elementary kaon production cross sections in baryon baryon reactions have been calculated using a one pion and one kaon exchange model. But their approach is still not fully consistent because they adopted the results of the pion baryon reactions from the resonance model [46], where the resonance model [46] does not include one kaon exchange in its basic assumptions. Thus, if one wants to be consistent with the parameters determined in the pion baryon reactions, one kaon exchange should not be introduced.

In Fig. 10 we show the energy dependence of the total cross sections for the $\Delta^{++}n \rightarrow p\Lambda K^+$ and $\Delta^-p \rightarrow n\Sigma^-K^+$ reactions, together with the data for the $pp \rightarrow p\Lambda K^+$, $pp \rightarrow p\Sigma^+K^0$ and $pp \rightarrow n\Sigma^+K^+$ reactions [49] plotted at the same excess energy above each threshold energy corresponding to the Λ and Σ production channels. The magnitude of the total cross section for the $\Delta^{++}n \rightarrow p\Lambda K^+$ reaction is almost equal to that of the $pp \rightarrow p\Lambda K^+$ reaction at the same excess energy just above the threshold, $\sqrt{s} - \sqrt{s_0} < 100$ MeV. However, at energies $\sqrt{s} - \sqrt{s_0} \simeq 1$ GeV, the magnitudes of both the $\Delta^{++}n \rightarrow p\Lambda K^+$ and $\Delta^-p \rightarrow n\Sigma^-K^+$ reactions become larger by about a factor of 6 than those of the $pp \rightarrow p\Lambda K^+$, and $pp \rightarrow p\Sigma^+K^0$ and $pp \rightarrow n\Sigma^+K^+$ reactions, respectively. One of the main reasons for this is the different spin structure of nucleon and Δ , as can be seen from Eq. (31), which produces different energy dependence in the Lorentz invariant scattering amplitude. (The difference in form factors and coupling constants is also the other reason.) Our result may be consistent with the conclusion that the $\Delta N \rightarrow NYK$ reactions give the largest contribution to kaon yield in heavy ion collisions. However, this should be explicitly checked.

The total cross sections for the other isospin channels of the $\Delta N \rightarrow NYK$ reactions are obtained by:

$$\begin{aligned} \sigma(\Delta^{++}n \rightarrow p\Lambda K^+) &= \sigma(\Delta^-p \rightarrow n\Lambda K^0) \\ = 3\sigma(\Delta^+p \rightarrow p\Lambda K^+) &= 3\sigma(\Delta^+n \rightarrow p\Lambda K^0) \\ = 3\sigma(\Delta^+n \rightarrow n\Lambda K^+) &= 3\sigma(\Delta^0p \rightarrow p\Lambda K^0) \\ = 3\sigma(\Delta^0p \rightarrow n\Lambda K^+) &= 3\sigma(\Delta^0n \rightarrow n\Lambda K^0), \end{aligned} \quad (44)$$

$$\begin{aligned} \sigma(\Delta^-p \rightarrow n\Sigma^-K^+) &= \sigma(\Delta^{++}n \rightarrow p\Sigma^+K^0) \\ = 2\sigma(\Delta^{++}n \rightarrow p\Sigma^0K^+) &= 2\sigma(\Delta^-p \rightarrow n\Sigma^0K^0) \\ = 3\sigma(\Delta^+n \rightarrow p\Sigma^-K^+) &= 3\sigma(\Delta^+p \rightarrow p\Sigma^+K^0) \\ = 3\sigma(\Delta^0p \rightarrow p\Sigma^-K^+) &= 3\sigma(\Delta^+n \rightarrow n\Sigma^+K^0) \\ = 3\sigma(\Delta^0n \rightarrow n\Sigma^-K^+) &= 3\sigma(\Delta^0p \rightarrow n\Sigma^+K^0) \\ = 6\sigma(\Delta^+p \rightarrow p\Sigma^0K^+) &= 6\sigma(\Delta^+n \rightarrow p\Sigma^0K^0) \\ = 6\sigma(\Delta^+n \rightarrow n\Sigma^0K^+) &= 6\sigma(\Delta^0p \rightarrow p\Sigma^0K^0) \\ = 6\sigma(\Delta^0p \rightarrow n\Sigma^0K^+) &= 6\sigma(\Delta^0n \rightarrow n\Sigma^0K^0). \end{aligned} \quad (45)$$

3.4 $\Delta N \rightarrow \Delta YK$

Similarly to the situation for the $NN \rightarrow \Delta YK$ reactions, the $\Delta\Delta \rightarrow \Delta YK$ reactions are not usually included in the simulation codes due to the high threshold energy. However, these reactions may be responsible for the low energy part of the kaon spectra. In Figs. 11 – 14, we

show energy dependence of the total cross sections sufficient for obtaining all isospin channels in the reactions, together with the experimental data of the $pp \rightarrow p\Lambda K^+$, $pp \rightarrow p\Sigma^0 K^+$, $pp \rightarrow p\Sigma^+ K^0$ and $pp \rightarrow n\Sigma^+ K^+$ reactions plotted at the same excess energies above the corresponding thresholds. The magnitudes of the total cross sections are almost equal to those measured for the $pp \rightarrow NYK$ reactions at the same excess energy, $\sqrt{s} - \sqrt{s_0} > 100$ MeV, with respect to each corresponding threshold, $\sqrt{s_0}$.

The total cross sections for the other isospin channels are obtained by:

$$\begin{aligned} \sigma(\Delta^{++}p \rightarrow \Delta^{++}\Lambda K^+) &= \sigma(\Delta^{++}n \rightarrow \Delta^{++}\Lambda K^0) \\ &= \sigma(\Delta^-p \rightarrow \Delta^-\Lambda K^+) = \sigma(\Delta^-n \rightarrow \Delta^-\Lambda K^0), \end{aligned} \quad (46)$$

$$\begin{aligned} 3\sigma(\Delta^+n \rightarrow \Delta^0\Lambda K^+) &= 3\sigma(\Delta^0p \rightarrow \Delta^+\Lambda K^0) \\ 4\sigma(\Delta^{++}n \rightarrow \Delta^+\Lambda K^+) &= 4\sigma(\Delta^+p \rightarrow \Delta^{++}\Lambda K^0) \\ 4\sigma(\Delta^0n \rightarrow \Delta^-\Lambda K^+) &= 4\sigma(\Delta^-p \rightarrow \Delta^0\Lambda K^0), \end{aligned} \quad (47)$$

$$\begin{aligned} \sigma(\Delta^+p \rightarrow \Delta^+\Lambda K^+) &= \sigma(\Delta^+n \rightarrow \Delta^+\Lambda K^0) \\ \sigma(\Delta^0p \rightarrow \Delta^0\Lambda K^+) &= \sigma(\Delta^0n \rightarrow \Delta^0\Lambda K^0), \end{aligned} \quad (48)$$

$$\begin{aligned} \sigma(\Delta^{++}n \rightarrow \Delta^{++}\Sigma^- K^+) &= \sigma(\Delta^{++}p \rightarrow \Delta^{++}\Sigma^+ K^0) \\ \sigma(\Delta^-n \rightarrow \Delta^-\Sigma^- K^+) &= \sigma(\Delta^-p \rightarrow \Delta^-\Sigma^+ K^0), \end{aligned} \quad (49)$$

$$\begin{aligned} 3\sigma(\Delta^0p \rightarrow \Delta^+\Sigma^- K^+) &= 3\sigma(\Delta^+n \rightarrow \Delta^0\Sigma^+ K^0) \\ 4\sigma(\Delta^+p \rightarrow \Delta^{++}\Sigma^- K^+) &= 4\sigma(\Delta^{++}n \rightarrow \Delta^+\Sigma^+ K^0) \\ 4\sigma(\Delta^-p \rightarrow \Delta^0\Sigma^- K^+) &= 4\sigma(\Delta^0n \rightarrow \Delta^-\Sigma^+ K^0), \end{aligned} \quad (50)$$

$$\begin{aligned} \sigma(\Delta^+n \rightarrow \Delta^+\Sigma^- K^+) &= \sigma(\Delta^+p \rightarrow \Delta^+\Sigma^+ K^0) \\ \sigma(\Delta^0n \rightarrow \Delta^0\Sigma^- K^+) &= \sigma(\Delta^0p \rightarrow \Delta^0\Sigma^+ K^0), \end{aligned} \quad (51)$$

$$\begin{aligned} \sigma(\Delta^{++}p \rightarrow \Delta^{++}\Sigma^0 K^+) &= \sigma(\Delta^{++}n \rightarrow \Delta^{++}\Sigma^0 K^0) \\ \sigma(\Delta^-p \rightarrow \Delta^-\Sigma^0 K^+) &= \sigma(\Delta^-n \rightarrow \Delta^-\Sigma^0 K^0), \end{aligned} \quad (52)$$

$$\begin{aligned} 3\sigma(\Delta^+n \rightarrow \Delta^0\Sigma^0 K^+) &= 3\sigma(\Delta^0p \rightarrow \Delta^+\Sigma^0 K^0) \\ 4\sigma(\Delta^{++}n \rightarrow \Delta^+\Sigma^0 K^+) &= 4\sigma(\Delta^+p \rightarrow \Delta^{++}\Sigma^0 K^0) \\ 4\sigma(\Delta^0n \rightarrow \Delta^-\Sigma^0 K^+) &= 4\sigma(\Delta^-p \rightarrow \Delta^0\Sigma^0 K^0), \end{aligned} \quad (53)$$

$$\begin{aligned} \sigma(\Delta^+p \rightarrow \Delta^+\Sigma^0 K^+) &= \sigma(\Delta^+n \rightarrow \Delta^+\Sigma^0 K^0) \\ \sigma(\Delta^0p \rightarrow \Delta^0\Sigma^0 K^+) &= \sigma(\Delta^0n \rightarrow \Delta^0\Sigma^0 K^0), \end{aligned} \quad (54)$$

$$\begin{aligned} 3\sigma(\Delta^+p \rightarrow \Delta^0\Sigma^+ K^+) &= 3\sigma(\Delta^0n \rightarrow \Delta^+\Sigma^- K^0) \\ 4\sigma(\Delta^{++}p \rightarrow \Delta^+\Sigma^+ K^+) &= 4\sigma(\Delta^+n \rightarrow \Delta^{++}\Sigma^- K^0) \\ 4\sigma(\Delta^0p \rightarrow \Delta^-\Sigma^+ K^+) &= 4\sigma(\Delta^-p \rightarrow \Delta^0\Sigma^0 K^0). \end{aligned} \quad (55)$$

3.5 $\Delta\Delta \rightarrow \Delta YK$

The energy dependence of the total cross sections for the $\Delta\Delta \rightarrow \Delta\Lambda K$ and $\Delta\Delta \rightarrow \Delta\Sigma K$ reactions are shown in Figs. 15, 16 and 17, together with the experimental data for the $pp \rightarrow p\Lambda K^+$ and $pp \rightarrow p\Sigma^0 K^+$ reactions plotted at the same excess energies above the corresponding hyperon production threshold. As expected, the magnitudes of the total cross sections for these reactions are small, because of the high threshold energies and three Δ 's are involved in the processes. The magnitudes for these reactions are almost 10 times smaller than those for the $pp \rightarrow p\Lambda K^+$ reaction which is shown in Fig. 17. The contributions from these reactions to the kaon yield in heavy ion collisions are therefore negligible.

The total cross sections for the other isospin channels are obtained by:

$$\begin{aligned} \sigma(\Delta^+\Delta^{++} \rightarrow \Delta^{++}\Lambda K^+) &= \sigma(\Delta^0\Delta^- \rightarrow \Delta^-\Lambda K^0) \\ = 3\sigma(\Delta^0\Delta^0 \rightarrow \Delta^-\Lambda K^+) &= 3\sigma(\Delta^+\Delta^+ \rightarrow \Delta^{++}\Lambda K^0) \\ = 9\sigma(\Delta^+\Delta^+ \rightarrow \Delta^+\Lambda K^+) &= 9\sigma(\Delta^0\Delta^0 \rightarrow \Delta^0\Lambda K^0), \end{aligned} \quad (56)$$

$$\sigma(\Delta^0\Delta^{++} \rightarrow \Delta^+\Lambda K^+) = \sigma(\Delta^+\Delta^- \rightarrow \Delta^0\Lambda K^0), \quad (57)$$

$$\sigma(\Delta^0\Delta^+ \rightarrow \Delta^0\Lambda K^+) = \sigma(\Delta^+\Delta^0 \rightarrow \Delta^+\Lambda K^0), \quad (58)$$

$$\begin{aligned} \sigma(\Delta^{++}\Delta^0 \rightarrow \Delta^{++}\Sigma^- K^+) &= \sigma(\Delta^{++}\Delta^0 \rightarrow \Delta^{++}\Sigma^0 K^0) \\ = \sigma(\Delta^{++}\Delta^- \rightarrow \Delta^+\Sigma^- K^+) &= \sigma(\Delta^{++}\Delta^- \rightarrow \Delta^+\Sigma^0 K^0) \\ = \sigma(\Delta^-\Delta^{++} \rightarrow \Delta^0\Sigma^0 K^+) &= \sigma(\Delta^-\Delta^{++} \rightarrow \Delta^0\Sigma^+ K^0) \\ = \sigma(\Delta^-\Delta^+ \rightarrow \Delta^-\Sigma^0 K^+) &= \sigma(\Delta^-\Delta^+ \rightarrow \Delta^-\Sigma^+ K^0), \end{aligned} \quad (59)$$

$$\begin{aligned} \sigma(\Delta^-\Delta^0 \rightarrow \Delta^-\Sigma^- K^+) &= \sigma(\Delta^{++}\Delta^+ \rightarrow \Delta^{++}\Sigma^+ K^0) \\ = 2\sigma(\Delta^+\Delta^{++} \rightarrow \Delta^{++}\Sigma^0 K^+) &= 2\sigma(\Delta^0\Delta^- \rightarrow \Delta^-\Sigma^0 K^0) \\ = 3\sigma(\Delta^+\Delta^+ \rightarrow \Delta^{++}\Sigma^- K^+) &= 3\sigma(\Delta^0\Delta^0 \rightarrow \Delta^-\Sigma^+ K^0) \\ = 6\sigma(\Delta^0\Delta^0 \rightarrow \Delta^-\Sigma^0 K^+) &= 6\sigma(\Delta^+\Delta^+ \rightarrow \Delta^{++}\Sigma^0 K^0) \\ = 9\sigma(\Delta^0\Delta^0 \rightarrow \Delta^0\Sigma^- K^+) &= 9\sigma(\Delta^+\Delta^+ \rightarrow \Delta^+\Sigma^+ K^0) \\ = 18\sigma(\Delta^+\Delta^+ \rightarrow \Delta^+\Sigma^0 K^+) &= 18\sigma(\Delta^0\Delta^0 \rightarrow \Delta^0\Sigma^0 K^0), \end{aligned} \quad (60)$$

$$\begin{aligned} 2\sigma(\Delta^0\Delta^{++} \rightarrow \Delta^+\Sigma^0 K^+) &= 2\sigma(\Delta^+\Delta^- \rightarrow \Delta^0\Sigma^0 K^0) \\ = 3\sigma(\Delta^0\Delta^+ \rightarrow \Delta^+\Sigma^- K^+) &= 3\sigma(\Delta^+\Delta^0 \rightarrow \Delta^0\Sigma^+ K^0), \end{aligned} \quad (61)$$

$$\begin{aligned} \sigma(\Delta^-\Delta^+ \rightarrow \Delta^0\Sigma^- K^+) &= \sigma(\Delta^{++}\Delta^0 \rightarrow \Delta^+\Sigma^+ K^0) \\ = 6\sigma(\Delta^0\Delta^+ \rightarrow \Delta^0\Sigma^0 K^+) &= 6\sigma(\Delta^+\Delta^0 \rightarrow \Delta^+\Sigma^0 K^0). \end{aligned} \quad (62)$$

4 Parametrizations

The energy dependence of the total cross sections calculated so far will be parametrized in the following form:

$$\sigma(B_1 B_2 \rightarrow B_3 YK) = a \left(\frac{s}{s_0} - 1 \right)^b \left(\frac{s_0}{s} \right)^c, \quad (63)$$

where s and s_0 are respectively the squares of the invariant collision energy and the threshold energy. a, b and c are the parameters to be determined so as to reproduce the calculated energy dependence of the total cross sections, with a in units of mb .

As was demonstrated in Ref. [61], the functional form, Eq. (63), can reproduce quite well the near-threshold behaviour of the total cross sections. The reason is that the function reflects the energy dependence of the phase space reasonably just above the threshold, where the energy dependence of the amplitude is usually weak. In addition the particles in the final state may be treated nonrelativistically due to the small amount of energy available. Assuming the relevant amplitude squared, $|T|^2$, to be a constant, the total cross section can be written as

$$\sigma = \frac{R_3}{F} |T|^2, \quad (64)$$

with R_3 the three-body phase space volume and F the flux factor. In Fig. 18 we show the results for the energy dependence of the total cross section for the $pp \rightarrow p\Lambda K^+$ reaction, calculated using Eq. (64), together with the experimental data [34, 49]. The square of the constant amplitude, $|T|^2$, was determined so as to fit the data point of COSY [34]. The parameter, b , which is mostly relevant to reproduce the shape of the energy dependence of the total cross section near the threshold, is obtained to be $b = 1.995$ in this case. This value of b gives a behaviour of the energy dependence very close to that of phase space in the nonrelativistic case [66]. On the other hand, the parameter, b , obtained to reproduce our results is, $b \simeq 2.000$, which is very close to the value of the above phase space calculation. The last term in Eq. (63), $(s_0/s)^c$, reflects both the energy dependence of the flux factor which becomes important at energies $\sqrt{s} - \sqrt{s_0} > 0.5$ GeV, and also the contribution from meson exchange which is expected to behave as s^{-2} .

The parameters, a, b and c in Eq. (63), determined so as to reproduce the results calculated in our model, are listed in Table 3. They are sufficient to reproduce all the isospin channels treated in the previous section. The corresponding threshold energies squared, s_0 , are also indicated.

Note that the parameters given in Table 3 are determined so as to reproduce the theoretical results at energies up to about 2 GeV above the corresponding threshold energies. The reason is, when kaon production is studied at energies larger than 2 GeV above threshold, we need to include more resonances which decay to kaon and hyperon in the model, as well as taking into account the other kaon production processes with more than three particles appearing in the final states, where it seems impossible due to the present experimental data available. In practice, we believe that the parametrizations are recommended to be used up to invariant collision energies about 3.6 GeV, which are usually enough.

Although we have parametrized explicitly all the isospin channels required, it has been traditional to use isospin-averaged cross sections. In order to compare our results with those isospin-averaged cross sections, we have also calculated them within the model. The results are again parametrized by the function, Eq. (63). The parameters, a, b and c , for the isospin-averaged cross sections, are listed in Table 4. Note that the parameterizations in Table 4 also

Table 3: Parameterizations for energy dependence of the total cross sections. a , b and c , appearing in Eq. (63) were determined so as to reproduce the calculated total cross sections at energies, $\sqrt{s} - \sqrt{s_0} < 2$ GeV, with \sqrt{s} and $\sqrt{s_0}$ being, respectively, the invariant collision energy and threshold energy. The parametrizations are recommended to be used up to invariant collision energy about 3.6 GeV.

No.	Reaction	s_0 (GeV 2)	a (mb)	b	c
1	$pp \rightarrow p\Lambda K^+$	6.504	1.879	2.176	5.264
2	$pn \rightarrow n\Lambda K^+$	6.504	2.812	2.121	4.893
3	$pp \rightarrow p\Sigma^0 K^+$	6.904	5.321	2.753	8.510
4	$nn \rightarrow n\Sigma^- K^+$	6.904	7.079	2.760	8.164
5	$pn \rightarrow n\Sigma^0 K^+$	6.904	6.310	2.773	7.820
6	$np \rightarrow p\Sigma^- K^+$	6.904	11.02	2.782	7.674
7	$pp \rightarrow n\Sigma^+ K^+$	6.904	1.466	2.743	3.271
8	$pp \rightarrow \Delta^- \Lambda K^+$	8.085	6.166	2.842	1.960
9	$pp \rightarrow \Delta^{++} \Sigma^- K^+$	8.531	10.00	2.874	2.543
10	$\Delta^{++} n \rightarrow p\Lambda K^+$	6.504	8.337	2.227	2.511
11	$\Delta^- p \rightarrow n\Sigma^- K^+$	6.904	52.72	2.799	6.303
12	$\Delta^{++} p \rightarrow \Delta^{++} \Lambda K^+$	8.085	2.704	2.303	5.551
13	$\Delta^+ n \rightarrow \Delta^0 \Lambda K^+$	8.085	0.312	2.110	2.165
14	$\Delta^+ p \rightarrow \Delta^+ \Lambda K^+$	8.085	2.917	2.350	6.557
15	$\Delta^{++} n \rightarrow \Delta^{++} \Sigma^- K^+$	8.531	10.33	2.743	8.915
16	$\Delta^0 p \rightarrow \Delta^+ \Sigma^- K^+$	8.531	2.128	2.843	5.986
17	$\Delta^+ n \rightarrow \Delta^+ \Sigma^- K^+$	8.531	10.57	2.757	10.11
18	$\Delta^{++} p \rightarrow \Delta^{++} \Sigma^0 K^+$	8.531	10.30	2.748	9.321
19	$\Delta^+ n \rightarrow \Delta^0 \Sigma^0 K^+$	8.531	1.112	2.846	5.943
20	$\Delta^+ p \rightarrow \Delta^+ \Sigma^0 K^+$	8.531	10.62	2.759	10.20
21	$\Delta^+ p \rightarrow \Delta^0 \Sigma^+ K^+$	8.531	0.647	2.830	3.862
22	$\Delta^+ \Delta^{++} \rightarrow \Delta^{++} \Lambda K^+$	8.085	1.054	2.149	7.969
23	$\Delta^0 \Delta^{++} \rightarrow \Delta^+ \Lambda K^+$	8.085	0.881	2.150	7.977
24	$\Delta^0 \Delta^+ \rightarrow \Delta^0 \Lambda K^+$	8.085	0.291	2.148	7.934
25	$\Delta^{++} \Delta^0 \rightarrow \Delta^{++} \Sigma^- K^+$	8.531	3.532	2.953	12.06
26	$\Delta^- \Delta^0 \rightarrow \Delta^- \Sigma^- K^+$	8.531	7.047	2.952	12.05
27	$\Delta^0 \Delta^{++} \rightarrow \Delta^+ \Sigma^0 K^+$	8.531	2.931	2.952	12.03
28	$\Delta^- \Delta^+ \rightarrow \Delta^0 \Sigma^- K^+$	8.531	5.861	2.952	12.04

Table 4: Parameterizations for the energy dependence of the isospin-averaged total cross sections. (See also the caption of Table 3.) For the K^+ production reactions, replace the values for the parameter a by $\frac{1}{2}a$.

No.	Reaction	a (mb)	b	c
1	$NN \rightarrow N\Lambda K$	2.330	2.140	5.024
2	$NN \rightarrow N\Sigma K$	15.49	2.768	7.222
3	$NN \rightarrow \Delta\Lambda K$	9.249	2.842	1.960
4	$NN \rightarrow \Delta\Sigma K$	12.50	2.874	2.543
5	$\Delta N \rightarrow N\Lambda K$	4.169	2.227	2.511
6	$\Delta N \rightarrow N\Sigma K$	39.54	2.799	6.303
7	$\Delta N \rightarrow \Delta\Lambda K$	2.679	2.280	5.086
8	$\Delta N \rightarrow \Delta\Sigma K$	21.18	2.743	8.407
9	$\Delta\Delta \rightarrow \Delta\Lambda K$	0.337	2.149	7.967
10	$\Delta\Delta \rightarrow \Delta\Sigma K$	5.140	2.952	12.05

include K^0 production channels. Thus, the parametrizations for the K^+ production channels alone can be obtained replacing the values for the parameter a in Table 4 by $\frac{1}{2}a$.

We show the energy dependence of the isospin-averaged total cross sections, $\bar{\sigma}$, calculated in the model for all the baryon baryon reactions in Fig. 19. Note that the horizontal axes indicate invariant collision energies. Our results illustrate that the magnitudes of the isospin-averaged cross sections at energies, $\sqrt{s} - \sqrt{s_0} < 200$ MeV, are, $\bar{\sigma}(\Delta N \rightarrow NYK) \simeq \bar{\sigma}(NN \rightarrow NYK)$ for both the Λ and Σ production channels. However, at energies, $\sqrt{s} - \sqrt{s_0} > 200$ MeV, the magnitudes of the cross sections $\bar{\sigma}(\Delta N \rightarrow NYK)$ become about 6 times larger than those of $\bar{\sigma}(NN \rightarrow \Delta YK)$. It is also noticeable that the magnitudes of $\bar{\sigma}(NN \rightarrow \Delta YK)$ become comparable with those of $\bar{\sigma}(NN \rightarrow NYK)$ at NN invariant energies about 3.1 GeV, and overcome factors of 5 to 10 at NN invariant energies about 3.5 GeV. In particular, this is pronounced for the Λ production reactions. It is not clear at the moment how much the $NN \rightarrow \Delta YK$ reactions contribute to the total kaon yield in heavy ion collisions because they have usually been neglected. It seems worthwhile to perform calculations including these reactions. At invariant energies larger than about 3.2 GeV, the magnitudes of $\bar{\sigma}(\Delta N \rightarrow \Delta YK)$ are also comparable to those of $\bar{\sigma}(NN \rightarrow NYK)$.

It is interesting to see if the relation for the elementary kaon production cross sections, $\bar{\sigma}(NN \rightarrow \Delta\Lambda K) > \bar{\sigma}(\Delta N \rightarrow N\Lambda K) > \bar{\sigma}(NN \rightarrow N\Lambda K)$, can appreciable influence inclusive kaon production in proton-nucleus or heavy ion collisions. If this is the case, high energy inclusive kaon production in heavy ion collisions will be also significantly influenced by the Δ . A test for this argument can be made by performing calculations for high energy inclusive kaon production both, neglecting all the Δ 's, and including them, and comparing the results with the existing experimental data.

Next, we compare the isospin-averaged total cross sections calculated in this model, with the commonly used relation suggested by Randrup and Ko [26]. For the $NN \rightarrow NYK$ reactions, they suggested the relations:

$$\bar{\sigma}(NN \rightarrow N\Lambda K) = 3 \sigma(pp \rightarrow p\Lambda K^+), \quad (65)$$

$$\bar{\sigma}(NN \rightarrow N\Sigma K) = 3 \left[\sigma(pp \rightarrow p\Sigma^0 K^+) + \sigma(pp \rightarrow p\Sigma^+ K^0) \right]. \quad (66)$$

In Fig. 20 we show the isospin-averaged total cross sections calculated in the model, $\bar{\sigma}(NN \rightarrow N\Lambda K)$ and $\bar{\sigma}(NN \rightarrow N\Sigma K)$ (denoted by our model), and the quantities calculated using the right hand side of Eqs. (65) and (66) (denoted by prescription from [26]). The explicit calculation shows disagreement of about a factor 2 between the relation suggested by Randrup and Ko [26] for most of the energy range up to 2 GeV above the thresholds, for both the Λ and Σ production reactions. Thus, the calculations performed using the relation suggested by Randrup and Ko [26] to obtain the isospin-averaged cross sections for the $NN \rightarrow NYK$ reactions, may have about a factor of 2 ambiguity for these reactions.

As for the $\Delta N \rightarrow NYK$ reactions, they suggested the relations [26]:

$$\bar{\sigma}(\Delta N \rightarrow N\Lambda K) = \frac{9}{4} \sigma(pp \rightarrow p\Lambda K^+), \quad (67)$$

$$\bar{\sigma}(\Delta N \rightarrow N\Sigma K) = \frac{9}{4} \left[\sigma(pp \rightarrow p\Sigma^0 K^+) + \sigma(pp \rightarrow p\Sigma^+ K^0) \right]. \quad (68)$$

In Fig. 21 we show similar quantities calculated within the present model as for the $NN \rightarrow NYK$ reactions. At energies near the thresholds, $\sqrt{s} - \sqrt{s_0} < 200$ MeV, our results are in good agreement with the relations Eqs. (67) and (68), suggested to obtain the isospin-averaged cross sections. However, at energies, $\sqrt{s} - \sqrt{s_0} \simeq 1$ GeV, our results show a factor of 6 discrepancy with the relations suggested by Randrup and Ko [26].

It is worth noting that the recent calculation for kaon production in heavy ion collisions in free space [35], performed at energies near or below the threshold region of the $NN \rightarrow N\Lambda K$ reaction, illustrates that the dominant contribution comes from the secondary, pion induced reactions. Cassing et al. [35] and Li and Ko [42] used the relations of Eqs. (65) – (68), to obtain the isospin-averaged cross sections. In view of our results, it seems necessary to perform calculations using the total cross sections parametrized in a consistent manner for both the baryon baryon and pion baryon reactions.

5 Application to heavy-ion collisions

Kaon production in heavy-ion collisions at SIS energies (1-2 AGeV) has been studied theoretically using various transport models. Important inputs for such studies are the elementary kaon production cross sections in pion baryon and baryon baryon interactions. Conclusions concerning nuclear matter equations of state and kaon in-medium properties, obtained by comparing calculations with measurements, depend on the input kaon production cross sections.

In Ref. [19], a detailed study of these elementary cross sections was carried out, based on both the parametrization of experimental data and theoretical model calculations. Here we want to compare the kaon yields in heavy-ion collisions obtained using the cross sections in this work with the cross sections of Ref. [19]. We will use the same relativistic transport model as in Ref. [19] so that the difference in kaon yield is due entirely to the different elementary cross sections used. In this way, we can get a feeling for the sensitivity of transport model predictions to the underlying elementary cross sections.

We take central Au+Au collisions at 1 AGeV and Ni+Ni collisions at 1.8 AGeV as examples. The results are shown in Figs. 22 and 23, respectively. From these figures, we can make the following observations:

1. Generally, the kaon yield obtained with the cross sections from this work is smaller than that obtained with cross sections from Ref. [19]. The difference is about a factor of two at 1 AGeV, and reduces to about 40% at 1.8 AGeV.
2. Using both sets of cross sections, the $N\Delta$ channel is found to make the largest contributions among all the baryon baryon interactions. This is also in agreement with the earlier findings using the simple Randrup-Ko parametrization.
3. The contribution from the $\Delta\Delta$ channel is particularly small using the cross sections from this work. This is due to the fact that in the present model, the cross section for $\Delta\Delta \rightarrow NYK$ channel is zero, while in Ref. [19] off-shell pion exchange was included and gave a small contribution.

6 Summary

Within the resonance model, which is fully relativistic, but includes only the tree-level processes as an effective and empirical contributions, we have studied the elementary kaon production reactions in baryon baryon collisions in a consistent manner with those for the pion baryon reactions. We have calculated and parametrized the energy dependence of the total cross sections for all the necessary isospin channels in the $NN \rightarrow NYK$, $NN \rightarrow \Delta YK$, $\Delta N \rightarrow NYK$, $\Delta N \rightarrow \Delta YK$ and $\Delta\Delta \rightarrow \Delta YK$ reactions ($Y = \Lambda$ and Σ). We have also calculated and parametrized those for the isospin-averaged cross sections and compared with the the relation suggested by Rundrup and Ko [26] to obtain the isospin-averaged cross sections.

The present study has several points which may need to be improved, for example, consistency with the unitarity, the possibility to add other types of meson exchanges, such as kaon exchange, and the overestimate for the $pn(np) \rightarrow NYK$ reactions and the reactions involving the Δ , we would like to emphasize a practical aspect of this work, which we believe providing a useful inputs for further investigations of kaon production in heavy ion collisions. Keeping these in mind, we state a few comments as follows. First, our explicit calculation indicates that the contributions from the $\Delta N \rightarrow NYK$ and $NN \rightarrow \Delta YN$ reactions are substantially larger than those from the $NN \rightarrow NYK$ reactions at higher energies. Second, the relation suggested by Randrup and Ko [26] (c.f. Eqs. (65) and (66)) deviates from our results by about a factor of 2 for the $NN \rightarrow NYK$ reactions. For the $\Delta N \rightarrow NYK$ reactions, the relation (c.f. Eqs. (67) and (68)) holds well at low energies, up to about 200 MeV above the threshold, but deviations by as much as a factor of 6 have emerged at higher energies. From these facts we conclude that it is necessary to use consistent parametrizations of total kaon production cross sections for both the pion baryon and baryon baryon reactions. Furthermore, one should use isospin-averaged total cross sections calculated in a consistent manner. Lastly although the present study has been made for exclusive kaon production, there might also be a significant difference between the ΔN and NN collision reactions in inclusive kaon production in proton-nucleus or heavy ion collisions. Thus, it is interesting to perform calculations for inclusive kaon production, focusing on the effect of the Δ .

Acknowledgement

We thank J. Haidenbauer for helpful comments on the unitarity and coupled channel calculation. K.T. would like to thank K. Yazaki for valuable discussions at the very early stage of this work. A.S. would like to thank W. Cassing and U. Mosel for valuable discussions. This work

was supported in part by the Forschungszentrum Jülich, the Australian Research Council, and the U.S. Department of Energy under grant No. DE-FG02-88ER40388.

7 Appendix

7.1 Coupling constants of the resonances

Here we give relations between the branching ratios of the adopted resonances and the corresponding coupling constants squared, evaluated in the rest frame of each resonance. Note that all the coupling constants appearing below should be understood as being multiplied by the appropriate form factors. In addition, the confidence level, spin and parity of each resonance is specified. For the definition of $\lambda(x, y, z)$ appearing below, see the text, after Eq. (34).

7.1.1 $N(1650)^{****}(\frac{1}{2})^-$

$$\begin{aligned} \Gamma(N(1650) \rightarrow N\pi) &= 3 \frac{g_{\pi NN(1650)}^2}{4\pi} \frac{(E_N + m_N)}{m_{N(1650)}} |\vec{p}_N|, \\ \text{with } |\vec{p}_N| &= \frac{\lambda^{1/2}(m_{N(1650)}^2, m_N^2, m_\pi^2)}{2m_{N(1650)}}, \end{aligned} \quad (69)$$

$$\begin{aligned} \Gamma(N(1650) \rightarrow N\eta) &= \frac{g_{\eta NN(1650)}^2}{4\pi} \frac{(E_N + m_N)}{m_{N(1650)}} |\vec{p}_N|, \\ \text{with } |\vec{p}_N| &= \frac{\lambda^{1/2}(m_{N(1650)}^2, m_N^2, m_\eta^2)}{2m_{N(1650)}}, \end{aligned} \quad (70)$$

$$\begin{aligned} \Gamma(N(1650) \rightarrow \Delta\pi) &= 2 \frac{g_{\pi\Delta N(1650)}^2}{6\pi} \frac{m_{N(1650)}(E_\Delta - m_\Delta)}{m_\pi^2 m_\Delta^2} |\vec{p}_\Delta|^3, \\ \text{with } |\vec{p}_\Delta| &= \frac{\lambda^{1/2}(m_{N(1650)}^2, m_\Delta^2, m_\pi^2)}{2m_{N(1650)}}, \end{aligned} \quad (71)$$

$$\begin{aligned} \Gamma(N(1650) \rightarrow \Lambda K) &= \frac{g_{\Lambda K N(1650)}^2}{4\pi} \frac{(E_\Lambda + m_\Lambda)}{m_{N(1650)}} |\vec{p}_\Lambda|, \\ \text{with } |\vec{p}_\Lambda| &= \frac{\lambda^{1/2}(m_{N(1650)}^2, m_\Lambda^2, m_K^2)}{2m_{N(1650)}}. \end{aligned} \quad (72)$$

7.1.2 $N(1710)^{***}(\frac{1}{2})^+$

$$\begin{aligned} \Gamma(N(1710) \rightarrow N\pi) &= 3 \frac{g_{\pi NN(1710)}^2}{4\pi} \frac{(E_N - m_N)}{m_{N(1710)}} |\vec{p}_N|, \\ \text{with } |\vec{p}_N| &= \frac{\lambda^{1/2}(m_{N(1710)}^2, m_N^2, m_\pi^2)}{2m_{N(1710)}}, \end{aligned} \quad (73)$$

$$\begin{aligned}\Gamma(N(1710) \rightarrow N\eta) &= \frac{g_{\eta NN(1710)}^2}{4\pi} \frac{(E_N - m_N)}{m_{N(1710)}} |\vec{p}_N|, \\ \text{with } |\vec{p}_N| &= \frac{\lambda^{1/2}(m_{N(1710)}^2, m_N^2, m_\eta^2)}{2m_{N(1710)}},\end{aligned}\tag{74}$$

$$\begin{aligned}\Gamma(N(1710) \rightarrow N\rho) &= 3 \frac{g_{\rho NN(1710)}^2}{4\pi} \frac{|\vec{p}_N|}{m_{N(1710)}} \left[E_N - 3m_N + E_\rho \left(\frac{m_{N(1710)}^2 - m_N^2}{m_\rho^2} - 1 \right) \right], \\ \text{with } |\vec{p}_N| &= \frac{\lambda^{1/2}(m_{N(1710)}^2, m_N^2, m_\rho^2)}{2m_{N(1710)}},\end{aligned}\tag{75}$$

$$\begin{aligned}\Gamma(N(1710) \rightarrow \Delta\pi) &= 2 \frac{g_{\pi\Delta N(1710)}^2}{6\pi} \frac{m_{N(1710)}(E_\Delta + m_\Delta)}{m_\pi^2 m_\Delta^2} |\vec{p}_\Delta|^3, \\ \text{with } |\vec{p}_\Delta| &= \frac{\lambda^{1/2}(m_{N(1710)}^2, m_\Delta^2, m_\pi^2)}{2m_{N(1710)}},\end{aligned}\tag{76}$$

$$\begin{aligned}\Gamma(N(1710) \rightarrow \Lambda K) &= \frac{g_{\Lambda K N(1710)}^2}{4\pi} \frac{(E_\Lambda - m_\Lambda)}{m_{N(1710)}} |\vec{p}_\Lambda|, \\ \text{with } |\vec{p}_\Lambda| &= \frac{\lambda^{1/2}(m_{N(1710)}^2, m_\Lambda^2, m_K^2)}{2m_{N(1710)}},\end{aligned}\tag{77}$$

$$\begin{aligned}\Gamma(N(1710) \rightarrow \Sigma K) &= 3 \frac{g_{\Sigma K N(1710)}^2}{4\pi} \frac{(E_\Sigma - m_\Sigma)}{m_{N(1710)}} |\vec{p}_\Sigma|, \\ \text{with } |\vec{p}_\Sigma| &= \frac{\lambda^{1/2}(m_{N(1710)}^2, m_\Sigma^2, m_K^2)}{2m_{N(1710)}}.\end{aligned}\tag{78}$$

7.1.3 $N(1720)^{****}(\frac{3}{2})^+$

$$\begin{aligned}\Gamma(N(1720) \rightarrow N\pi) &= 3 \frac{g_{\pi NN(1720)}^2}{12\pi} \frac{(E_N + m_N)}{m_{N(1720)} m_\pi^2} |\vec{p}_N|^3, \\ \text{with } |\vec{p}_N| &= \frac{\lambda^{1/2}(m_{N(1720)}^2, m_N^2, m_\pi^2)}{2m_{N(1720)}},\end{aligned}\tag{79}$$

$$\begin{aligned}\Gamma(N(1720) \rightarrow N\eta) &= 3 \frac{g_{\pi NN(1720)}^2}{12\pi} \frac{(E_N + m_N)}{m_{N(1720)} m_\eta^2} |\vec{p}_N|^3, \\ \text{with } |\vec{p}_N| &= \frac{\lambda^{1/2}(m_{N(1720)}^2, m_N^2, m_\eta^2)}{2m_{N(1720)}},\end{aligned}\tag{80}$$

$$\begin{aligned}\Gamma(N(1720) \rightarrow N\rho) &= 3 \frac{g_{\rho NN(1720)}^2}{12\pi} \frac{(E_N - m_N)}{m_{N(1720)}} \left[3 + \frac{\vec{p}_N^2}{m_\rho^2} \right] |\vec{p}_N|, \\ \text{with } |\vec{p}_N| &= \frac{\lambda^{1/2}(m_{N(1720)}^2, m_N^2, m_\rho^2)}{2m_{N(1720)}},\end{aligned}\tag{81}$$

$$\begin{aligned}\Gamma(N(1720) \rightarrow \Delta\pi) &= 2 \frac{g_{\pi\Delta N(1720)}^2}{36\pi} \frac{m_\Delta |\vec{p}_\Delta|}{m_{N(1720)}} \left[\left(\frac{E_\Delta}{m_\Delta} \right) - 1 \right] \left[2 \left(\frac{E_\Delta}{m_\Delta} \right)^2 - 2 \left(\frac{E_\Delta}{m_\Delta} \right) + 5 \right], \\ \text{with } |\vec{p}_\Delta| &= \frac{\lambda^{1/2}(m_{N(1720)}^2, m_\Delta^2, m_\pi^2)}{2m_{N(1720)}},\end{aligned}\tag{82}$$

$$\begin{aligned}\Gamma(N(1720) \rightarrow \Lambda K) &= \frac{g_{K\Lambda N(1720)}^2}{12\pi} \frac{(E_\Lambda + m_\Lambda)}{m_{N(1720)} m_K^2} |\vec{p}_\Lambda|^3, \\ \text{with } |\vec{p}_\Lambda| &= \frac{\lambda^{1/2}(m_{N(1720)}^2, m_\Lambda^2, m_K^2)}{2m_{N(1720)}},\end{aligned}\tag{83}$$

$$\begin{aligned}\Gamma(N(1720) \rightarrow \Sigma K) &= 3 \frac{g_{K\Sigma N(1720)}^2}{12\pi} \frac{(E_\Sigma + m_\Sigma)}{m_{N(1720)} m_K^2} |\vec{p}_\Sigma|^3, \\ \text{with } |\vec{p}_\Sigma| &= \frac{\lambda^{1/2}(m_{N(1720)}^2, m_\Sigma^2, m_K^2)}{2m_{N(1720)}}.\end{aligned}\tag{84}$$

7.1.4 $\Delta(1920)^{***}(\frac{3}{2})^+$

$$\begin{aligned}\Gamma(\Delta(1920) \rightarrow N\pi) &= \frac{g_{\pi N \Delta(1920)}^2}{12\pi} \frac{(E_N + m_N)}{m_{\Delta(1920)} m_\pi^2} |\vec{p}_N|^3, \\ \text{with } |\vec{p}_N| &= \frac{\lambda^{1/2}(m_{\Delta(1920)}^2, m_N^2, m_\pi^2)}{2m_{\Delta(1920)}},\end{aligned}\tag{85}$$

$$\begin{aligned}\Gamma(\Delta(1920) \rightarrow \Sigma K) &= \frac{g_{\pi N \Delta(1920)}^2}{12\pi} \frac{(E_\Sigma + m_\Sigma)}{m_{\Delta(1920)} m_K^2} |\vec{p}_\Sigma|^3, \\ \text{with } |\vec{p}_\Sigma| &= \frac{\lambda^{1/2}(m_{\Delta(1920)}^2, m_\Sigma^2, m_K^2)}{2m_{\Delta(1920)}}.\end{aligned}\tag{86}$$

7.2 Cross section relation for the $\pi N \rightarrow \Lambda K$ reactions

Here, we add a relation for the total cross sections for the $\pi N \rightarrow \Lambda K$ reactions, which was not mentioned in Ref. [46]. The relation is:

$$\begin{aligned}\sigma(\pi^+ n \rightarrow \Lambda K^+) &= \sigma(\pi^- p \rightarrow \Lambda K^0) \\ = 2\sigma(\pi^0 p \rightarrow \Lambda K^+) &= 2\sigma(\pi^0 n \rightarrow \Lambda K^0).\end{aligned}\tag{87}$$

References

- [1] W. Cassing, V. Metag, U. Mosel and K. Niita, Phys. Rep. 188 (1990) 363.
- [2] U. Mosel, Annu. Rev. Nucl. Part. Sci. 41 (1991) 29.
- [3] V. Metag, Prog. Part. Nucl. Phys. 30 (1993) 75.
- [4] E. Grosse, Prog. Part. Nucl. Phys. 30 (1993) 89.
- [5] S. Schnetzer et al., Phys. Rev. Lett. 49 (1982) 989.
- [6] S. Nagamiya, Phys. Rev. Lett. 49 (1982) 1383.
- [7] J. Aichelin and C. M. Ko, Phys. Rev. Lett. 55 (1985) 2661.
- [8] B. Schürmann and W. Zwermann, Phys. Lett. B 183 (1987) 31.
- [9] L. Xiong, C. M. Ko, and J. Q. Wu, Phys. Rev. C 42 (1990) 2231.
- [10] A. Lang, W. Cassing, U. Mosel and K. Weber, Nucl. Phys. A 541 (1992) 507.
- [11] G. Q. Li and C. M. Ko, Phys. Lett. B 349 (1995) 405.
- [12] P. Koch, B. Müller and J. Rafelski, Phys. Rep. 142 (1986) 167, and references therein; C.M. Ko and L. Xia, Nucl Phys. A 498 (1989) 561c; R. Mattiello, H. Sorge, H. Stöcker, and W. Greiner, Phys. Rev. Lett. 63 (1989) 1459.
- [13] T. Abbot et al., Phys. Rev. Lett. 64 (1990) 847.
- [14] G. E. Brown, C. M. Ko, Z. G. Wu and L. H. Xia, Phys. Rev. C 43 (1991) 1881; C. M. Ko, Z. G. Wu, L. H. Xia and G. E. Brown, Phys. Rev. Lett. 66 (1991) 2577; G. E. Brown, C. M. Ko, and K. Kubodera, Z. Phys. A 341 (1992) 301.
- [15] V. Koch, Phys. Lett. B 351 (1995) 29
- [16] G. E. Brown, M. Rho, Phys. Rep. 269 (1996) 333.
- [17] C. Hartnack, J. Aichelin, H. Stöcker and W. Greiner, Phys. Rev. Lett. 72 (1994) 3767.
- [18] H. Stöcker and W. Greiner, Phys. Rep. 137 (1986) 277, and references therein.
- [19] G.Q. Li, C.H. Lee and G.E. Brown, Nucl. Phys. A 625 (1997) 435, and references therein; nucl-th/9709024; Phys. Rev. Lett. 79 (1997) 5214.
- [20] J. Aichelin et al., Phys. Rev. Lett. 58 (1987) 1926.
- [21] G.Q. Li et al., Nucl. Phys. A 537 (1992) 645.
- [22] T. Maruyama et al., Nucl. Phys. A 573 (1994) 653.
- [23] X.S. Fang, C.M. Ko and Y.M. Zheng, Nucl. Phys. A 556 (1993) 499; C.M. Ko, X.S. Fang and Y.M. Zheng, International workshop XXI on Gross properties of nuclei and nuclear excitations, ed. by H. Ferdmeier, (1993) 29.

- [24] J.Q. Wu and C.M. Ko, Nucl. Phys. A 499 (1989) 810.
- [25] X.S. Fang, C.M. Ko, G.Q. Li and Y.M. Zheng, Phys. Rev. C 49 (1994) 608.
- [26] J. Randrup and C.M. Ko, Nucl. Phys. A 343 (1980) 519; Nucl. Phys. A 411 (1983) 537.
- [27] J. Cugnon and R. M. Lombard, Nucl. Phys. A 422 (1984) 635; J. Cugnon and R. M. Lombard, Phys. Lett B 134B (1984) 392.
- [28] E. Ferrari, Nuovo Cim. 13 (1959) 1285; 15 (1960) 652; Phys. Rev. 120 (1960) 988.
- [29] Tsu Yao, Phys. Rev. 125 (1962) 1048.
- [30] A. Deloff, Nucl. Phys. A 505 (1989) 583.
- [31] J.M. Laget, Phys. Lett. B259 (1991) 24.
- [32] A.A. Sibirtsev, Sov. J. Nucl. Phys. 55 (1992) 145; A.A. Sibirtsev, M. Büscher, Z. Phys. A 347 (1994) 191.
- [33] D. Miśkowiec et al. (for KaoS collaboration), Phys. Rev. Lett. 72 (1994) 3650; W. Ahner et al., Z. Phys. A 341 (1991) 123.
- [34] J.T. Balewski et al., Phys. Lett. B 338 (1996) 859; J.T. Balewski et al., nucl-ex/9803003; W. Oelert, nucl-ex/9803004
- [35] W. Cassing, E.L. Bratkovskaya, U. Mosel, S. Teis and A. Sibirtsev, Nucl. Phys. A 614 (1997) 415.
- [36] C. Fuchs et al., Phys. Rev. C 56 (1997) R606; Z.S. Wang et al., Phys. Rev. Lett. (1997) 4096.
- [37] M. Debowski et al., Z. Phys. A 356 (1996) 313; Phys. Lett. B 413 (1997) 8.
- [38] A.A. Sibirtsev, Phys. Lett. B 359 (1995) 29.
- [39] S.W. Huang et al., Phys. Lett. B 298 (1993) 41.
- [40] C. Hartnack, J. Jaenicke, L. Sehn, H. Stöcker, J. Aichelin, Nucl. Phys. A 580 (1994) 643.
- [41] Bao-An Li, Phys. Rev. C 50 (1994) 2144.
- [42] G.Q. Li and C.M. Ko, Nucl. Phys. A 594 (1995) 439.
- [43] T. Fuester and U. Mosel, nucl-th/9708051; G. Penner, T. Fuester and U. Mosel, nucl-th/9802010.
- [44] K. Tsushima, A. Sibrtsev, A. W. Thomas, Phys. Lett. B 390 (1997) 29.
- [45] A. Sibrtsev, K. Tsushima, A. W. Thomas, nucl-th/9711028 to appear in Phys. Lett. B.
- [46] K. Tsushima, S.W. Huang and Amand Faessler, Phys. Lett. B 337 (1994) 245; J. Phys. G21 (1995) 33; in proceedings *Joint Japan-Australia Workshop on Quarks, Hadrons and Nuclei*, Adelaide, South Australia, November 15-24 (1995), nucl-th/9602005; Australian. J. Phys. 50 (1997) 35.

- [47] R. Bilger et al., Phys. Lett. B 420 (1998) 217.
- [48] G.Q. Li and C.M. Ko, Nucl. Phys. A 594 (1995) 460.
- [49] A. Baldini, V. Flaminio, W.G. Moorhead and D.R.O. Morrison, *Landolt-Börnstein, Numerical Data and Functional Relationships in Science and Technology*, vol. 12, ed. by H. Schopper, Springer-Verlag (1988), *Total Cross Sections of High Energy Particles*.
- [50] R.E. Ansorge et al., Nucl. Phys. B103 (1976) 509.
- [51] G. Fäldt and C. Wilkin, Z. Phys. A 357 (1997) 241.
- [52] A. Sibirtsev and W. Cassing, nucl-th/9802025.
- [53] G.F. Bertsch and S. Das Gupta, Phys. Rep. 160 (1988) 189.
- [54] W. Zwermann, B. Schürmann, K. Dietrich and E. Martschew, Phys. Lett. B 134 (1984) 397, W. Zwermann, B. Schürmann, Nucl. Phys. A 423 (1984) 525.
- [55] W. Cassing et al., Z. Phys. A349 (1994) 77.
- [56] H. W. Barz and H. Iwe, Phys. Lett. B 143 (1984) 55; Nucl Phys. A 453 (1986) 728.
- [57] X. S. Fang, C. M. Ko, G. Q. Li and Y. M. Zheng, Nucl. Phys. A 575 (1994) 766.
- [58] H. Sorge, H. Stöcker and W. Greiner, Ann. Phys. (NY) 192 (1989) 266.
- [59] J. Aichelin, Phys. Rep. 202 (1991) 235.
- [60] V.N. Russkikh and Yu.B. Ivanov, Nucl. Phys. A 543 (1992) 751.
- [61] A.A. Sibirtsev, Nucl. Phys. A 604 (1996) 455; A. Sibirtsev, W. Cassing and U. Mosel, Z. Phys. A 358 (1997) 357.
- [62] G.Q. Li , C.M. Ko and W.S. Chung, Phys. Rev. C 57 (1998) 434.
- [63] Particle Data Group, Phys. Rev. D 50 (1994).
- [64] R. Machleidt, Adv. Nucl. Phys. 19 (1989) 189.
- [65] V. Barger and R. Phillips, *Collider Physics*, Addison-Wesley Publishing Company (1987).
- [66] E. Byckling, K. Kajantie, *Particle Kinematics*, John Wiley & Sons (1973).

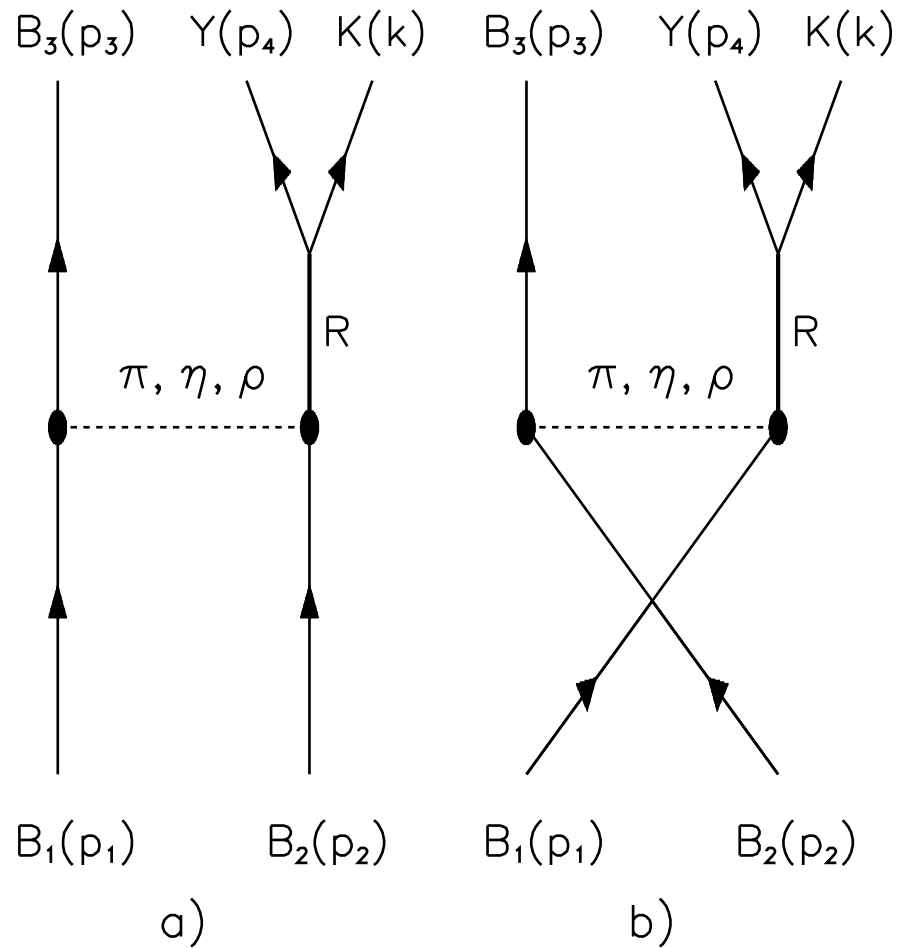


Figure 1: Kaon production processes in the resonance model. B_i ($i = 1, 2, 3$), Y and R stand for respectively, either the nucleon or the Δ , either the Λ or the Σ hyperon, and the baryon resonances.

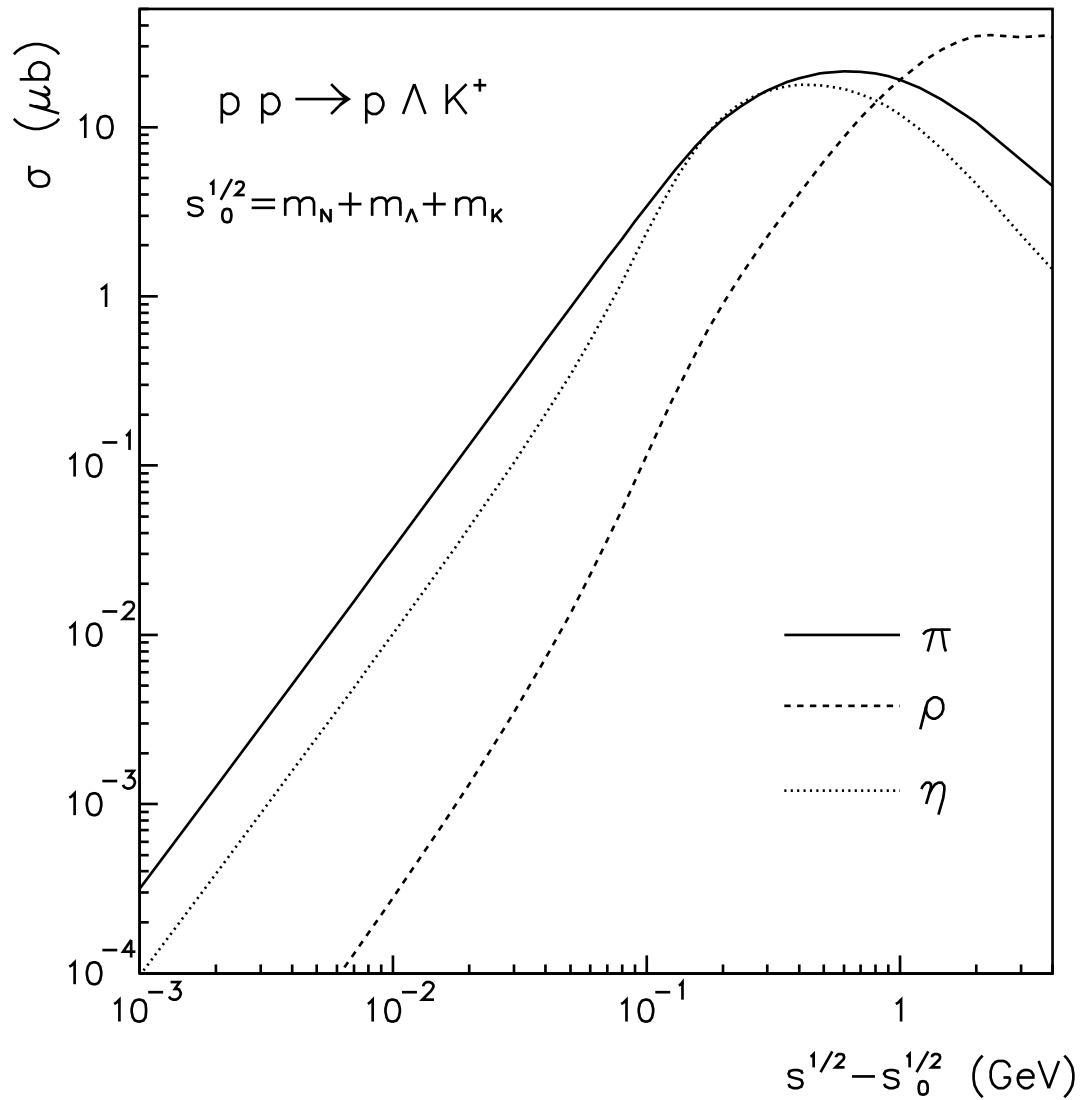


Figure 2: Separate contributions from π , ρ and η -exchanges to the total cross section for the $pp \rightarrow p\Lambda K^+$ reaction. $s^{1/2}$ and $s_0^{1/2} = m_N + m_\Lambda + m_K$ are the invariant collision energy and threshold energy, respectively.

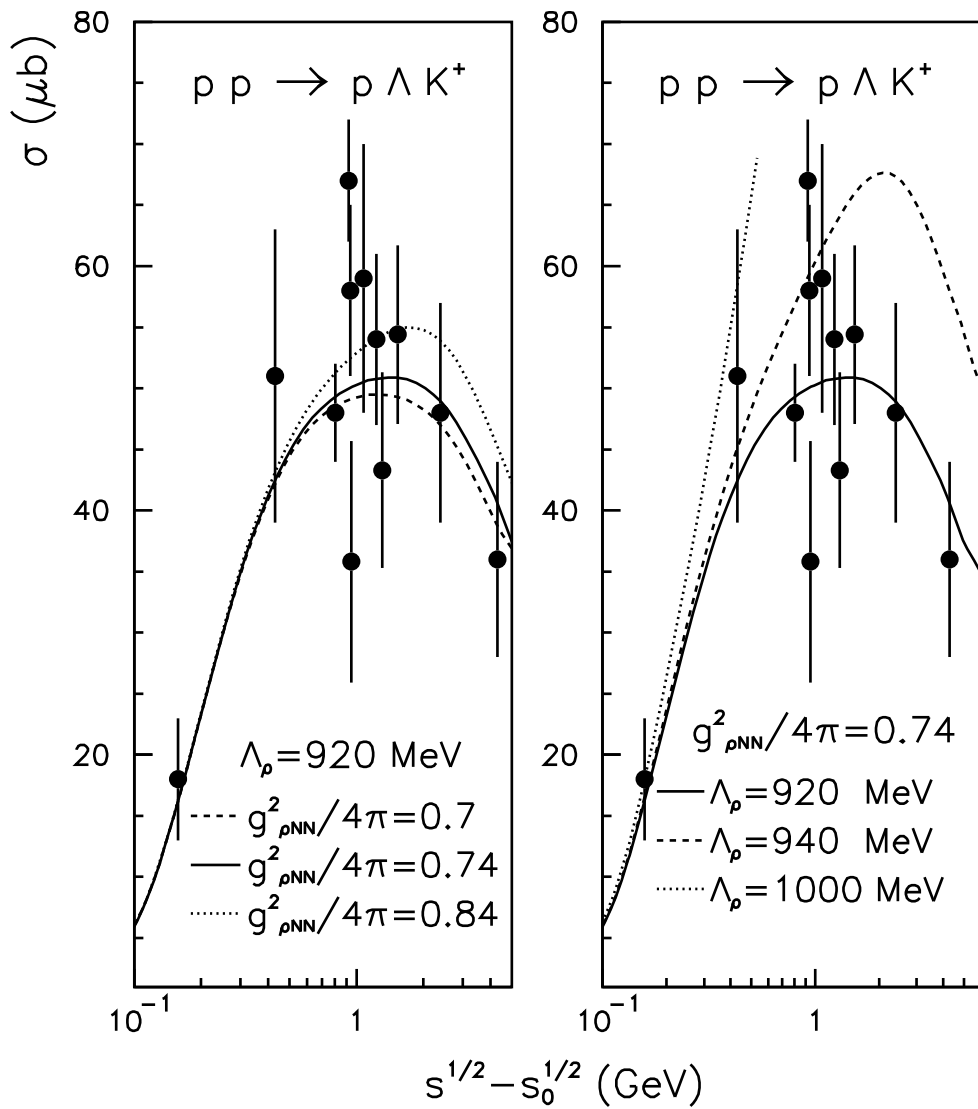


Figure 3: Dependence on the ρNN coupling constant and cut-off parameter of the total cross section for the $pp \rightarrow p\Lambda K^+$ reaction. The dots show experimental data from Ref. [49].

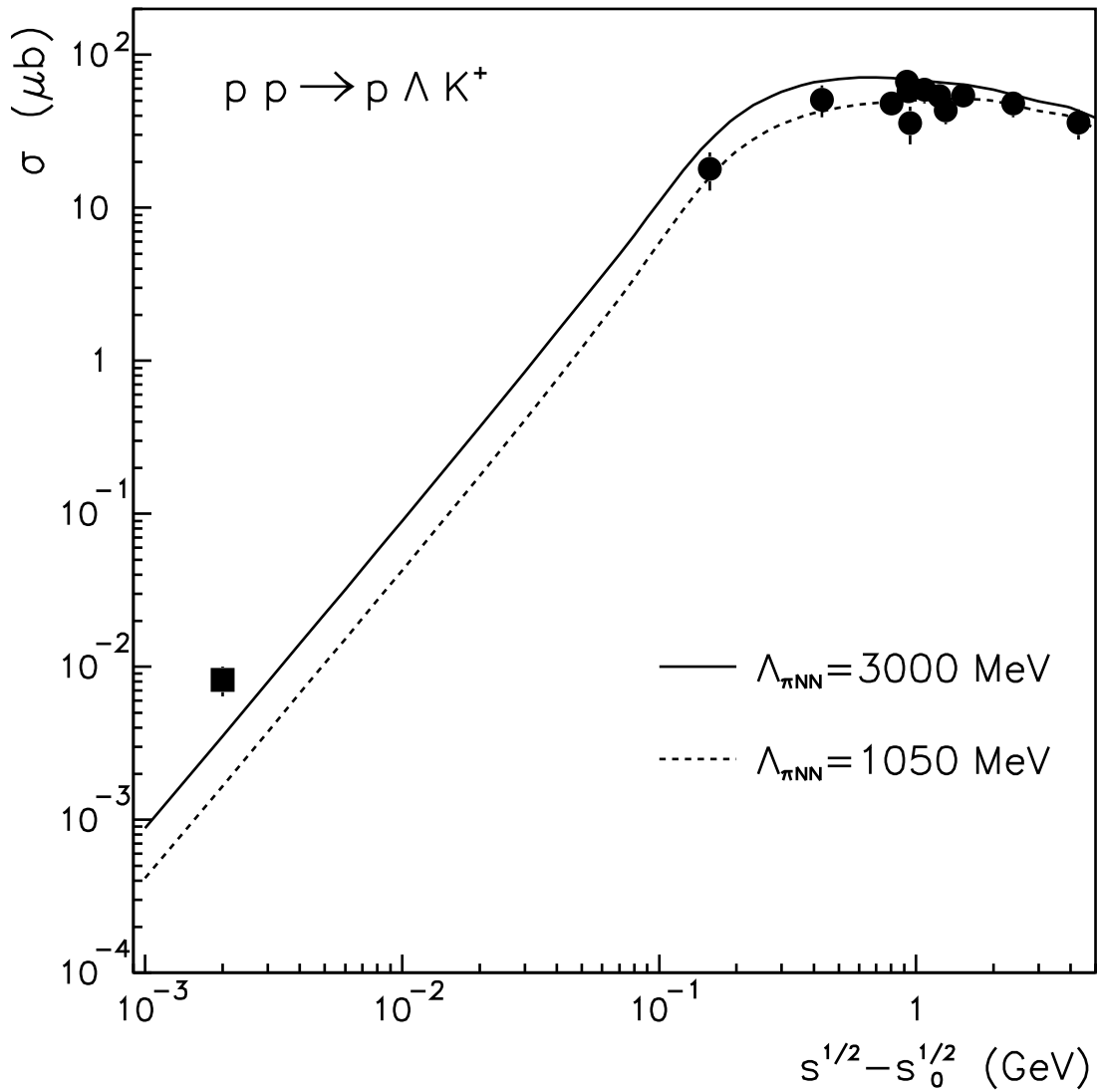


Figure 4: Dependence on the cut-off parameter in the πNN form factor, $\Lambda_{\pi NN}$, of the total cross sections for the $pp \rightarrow p\Lambda K^+$ reaction. The dots and square are the experimental data respectively from Ref. [49] and Ref. [34].

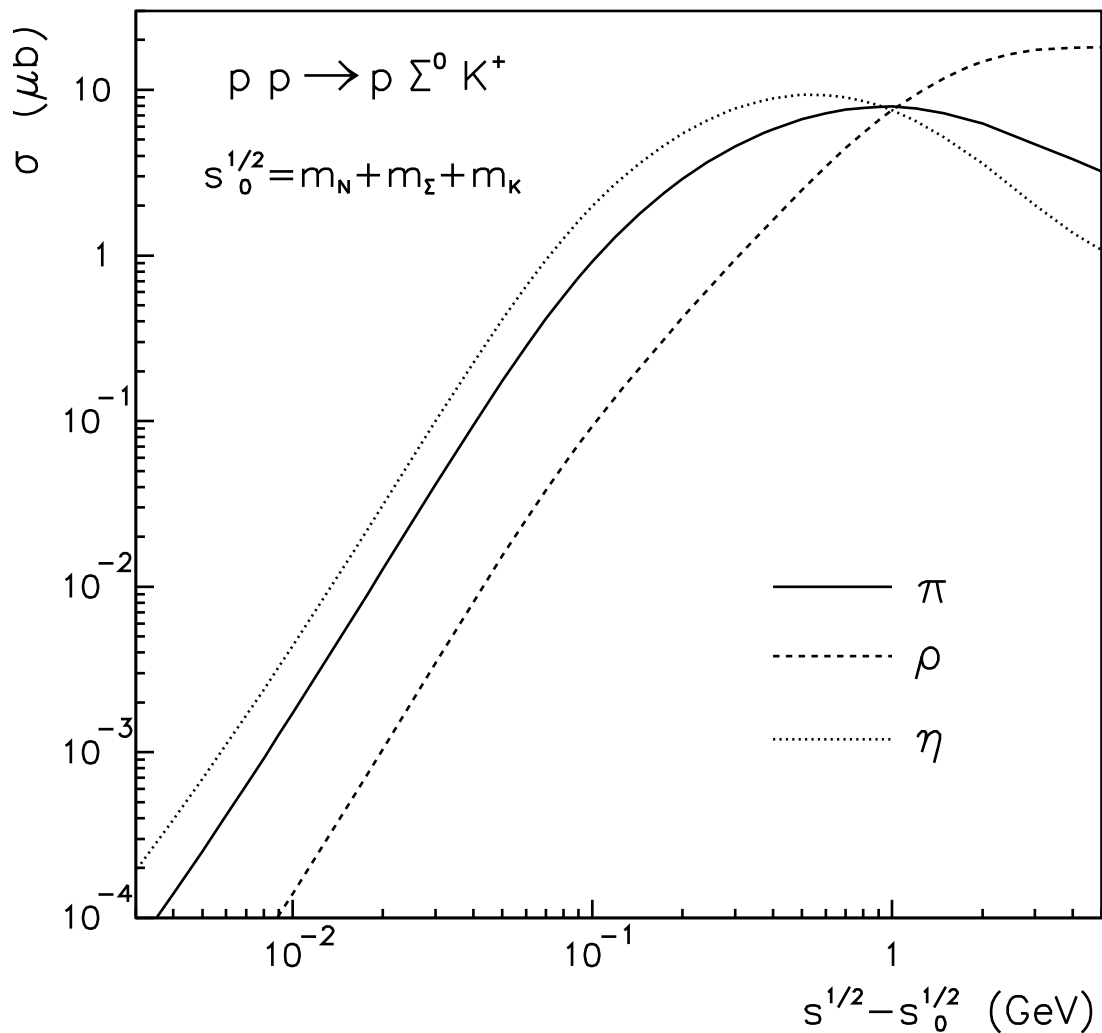


Figure 5: Separate contributions from π , ρ and η -exchanges to the total cross sections for the $pp \rightarrow p\Sigma^0 K^+$ reaction.

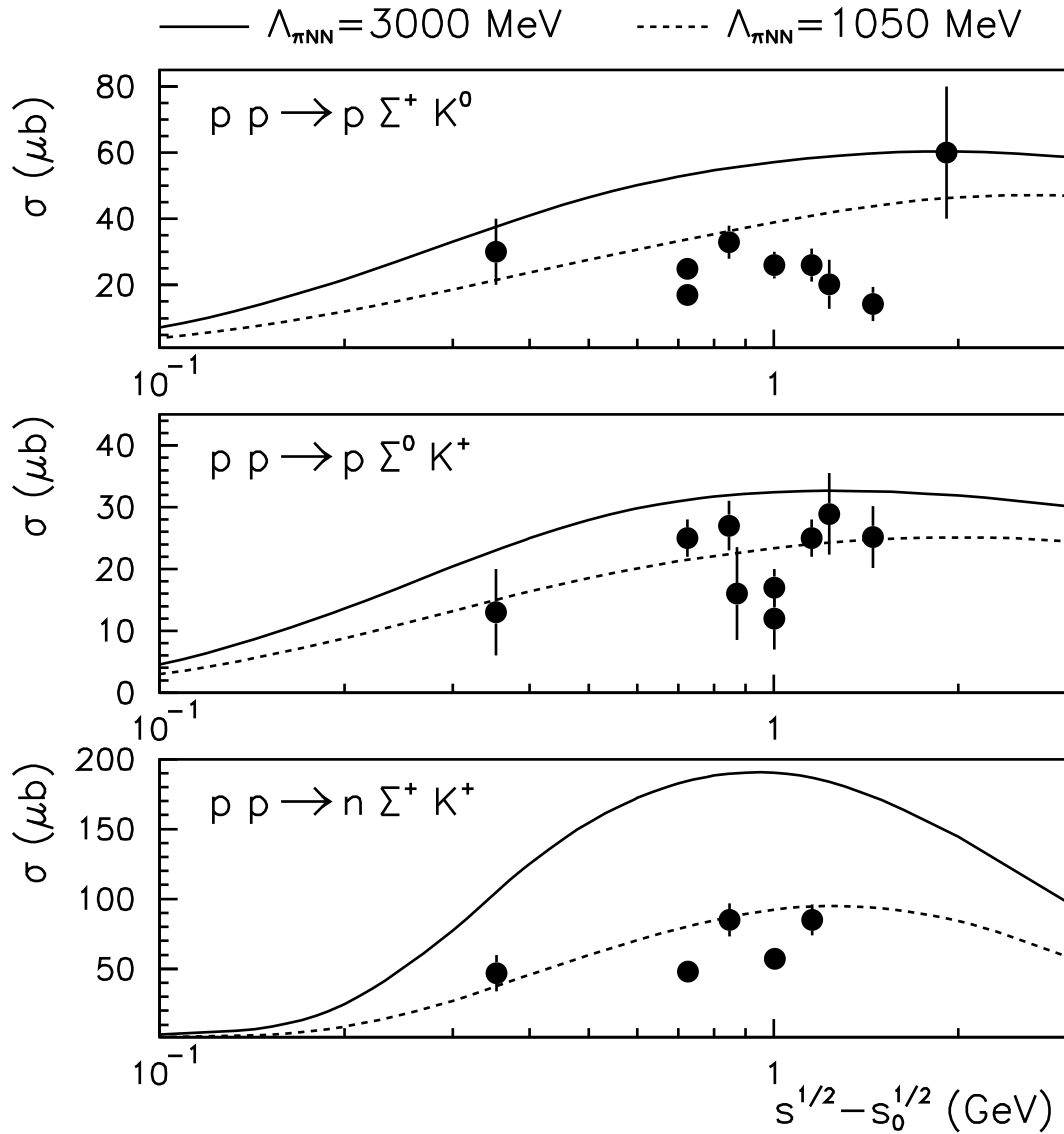


Figure 6: Energy dependence of the total cross sections for the $pp \rightarrow p\Sigma^+K^0$, $pp \rightarrow p\Sigma^0K^+$ and $pp \rightarrow n\Sigma^+K^+$ reactions. The dots stand for the experimental data from Ref. [49] with error bars. The solid and dashed lines show our results calculated using different values for the cut-off parameter, $\Lambda_{\pi NN} = 3000$ MeV and 1050 MeV, respectively.

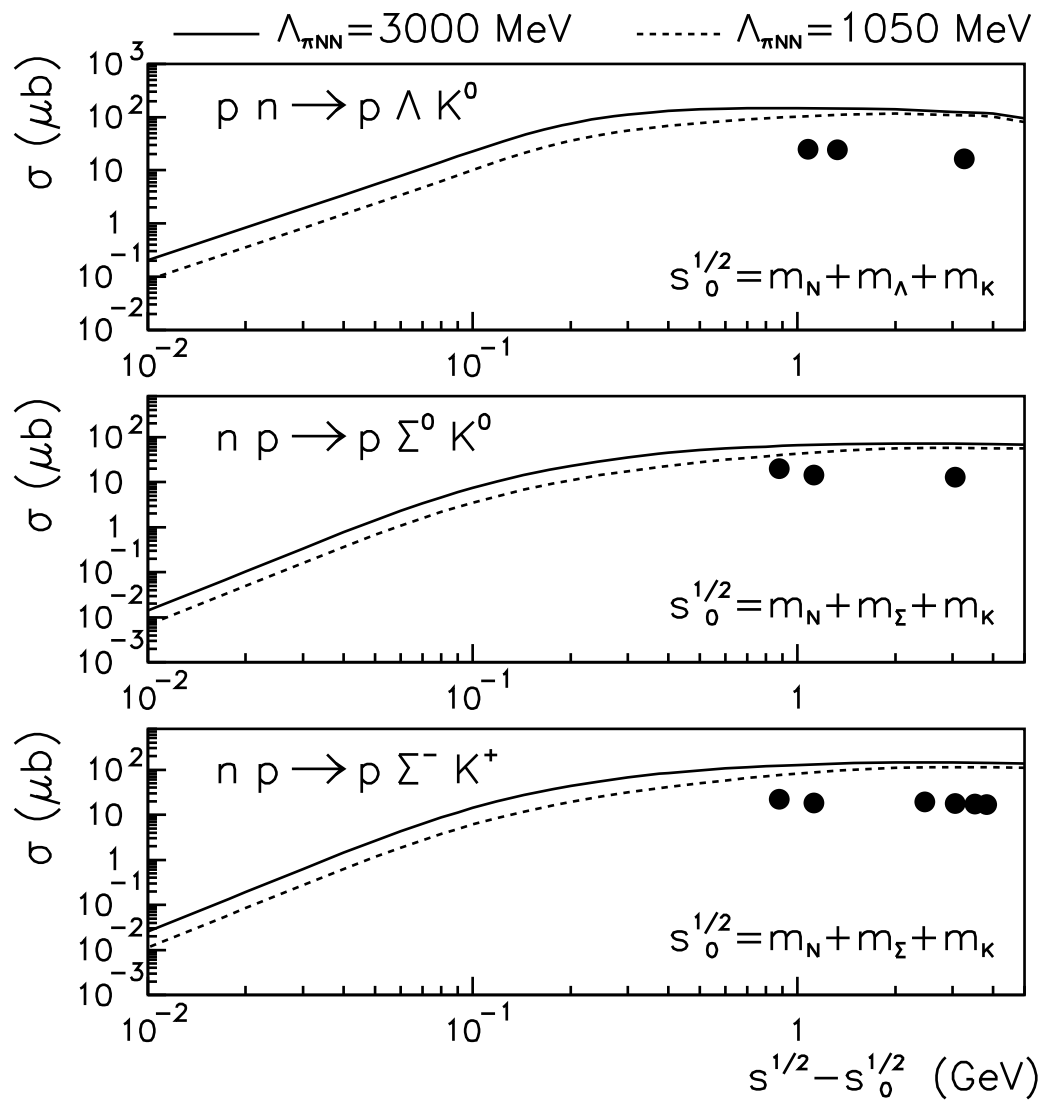


Figure 7: Same as in Fig. 6, but for the $p\bar{n} \rightarrow p\Lambda K^0$, $n\bar{p} \rightarrow p\Sigma^0 K^0$ and $n\bar{p} \rightarrow p\Sigma^- K^+$ reactions. Error bars are smaller than the dots.

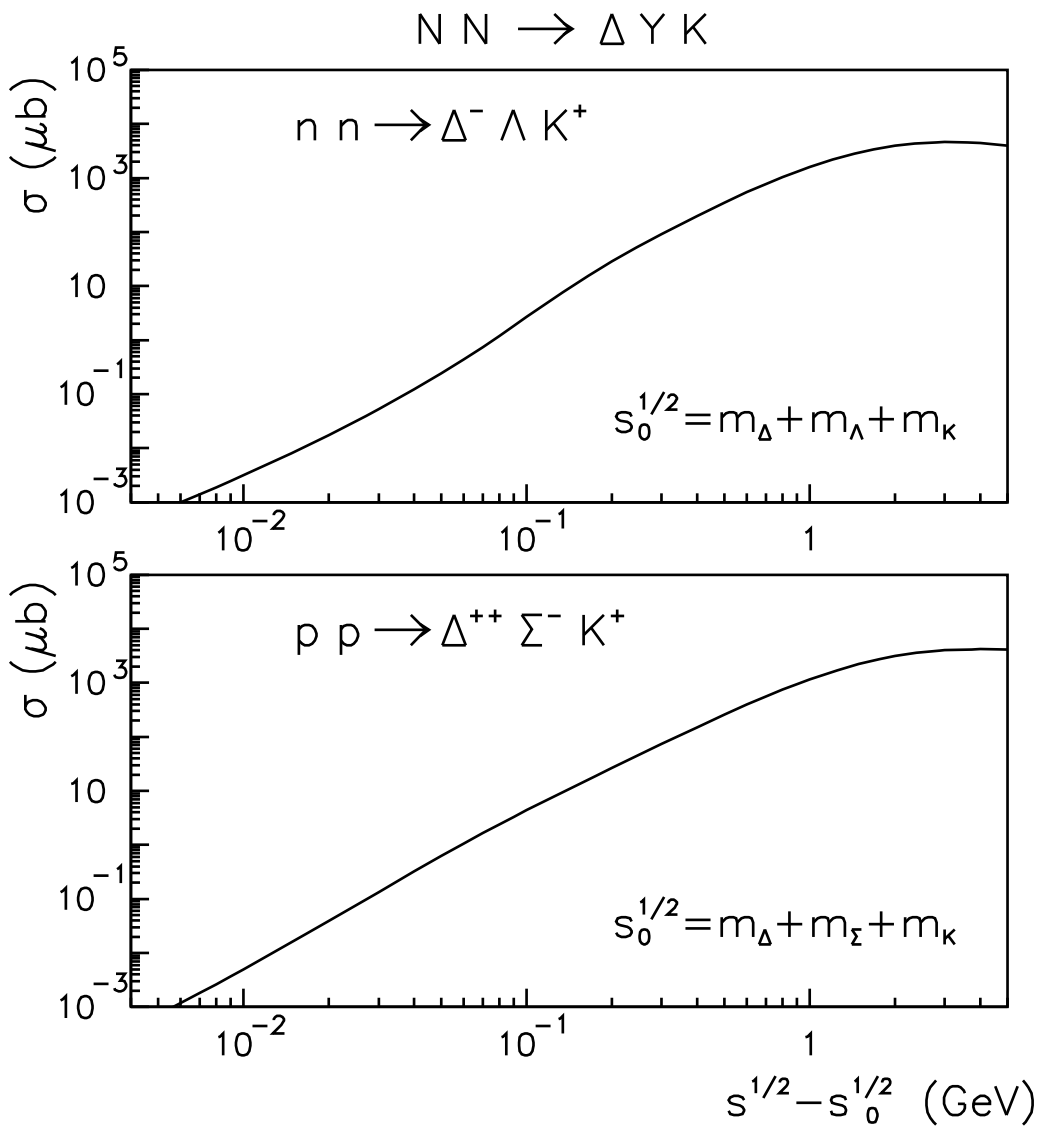


Figure 8: Energy dependence of the total cross sections for the $nn \rightarrow \Delta^- \Lambda K^+$ and $pp \rightarrow \Delta^{++} \Sigma^- K^+$ reactions.

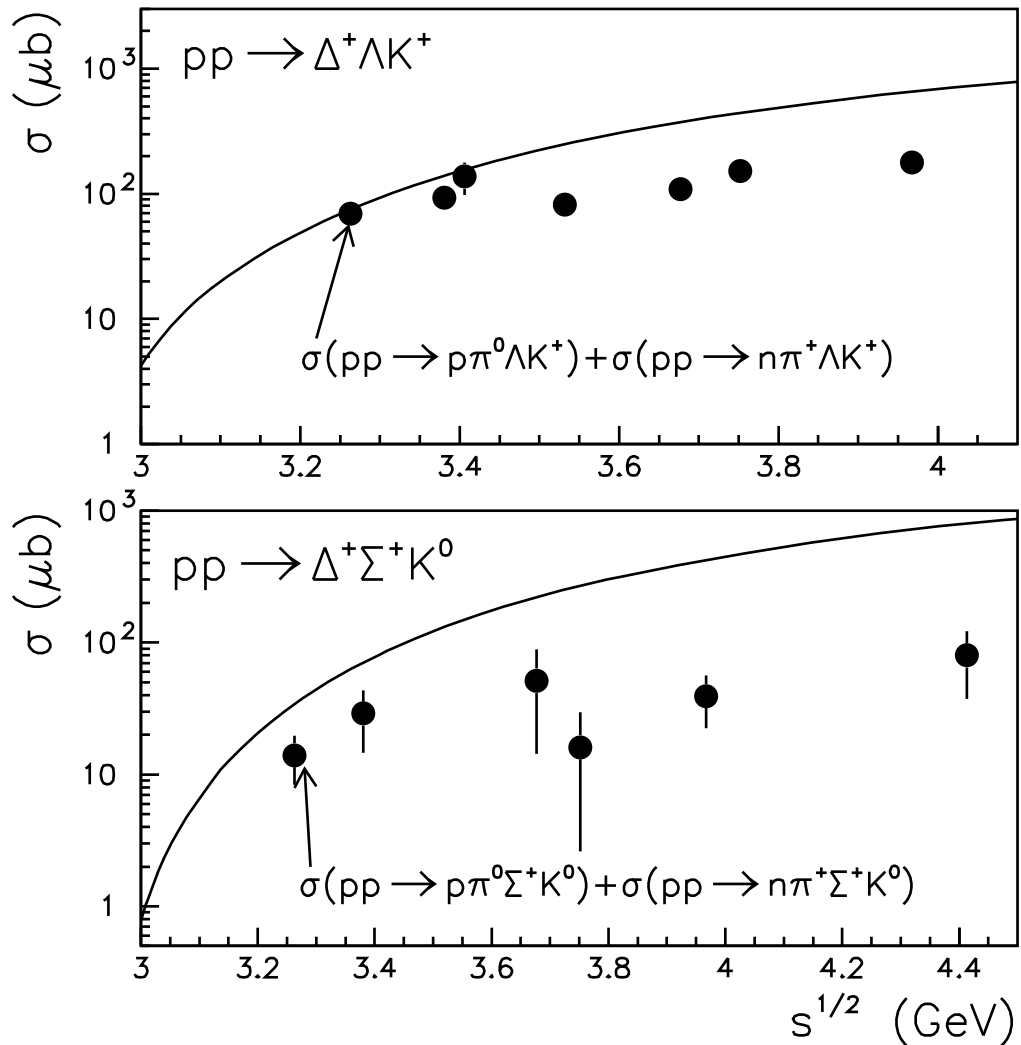


Figure 9: Comparison of the energy dependence of the total cross sections for the $pp \rightarrow \Delta Y K$ and $pp \rightarrow N \pi Y K$ reactions. Note that the parametrizations are recommended to be used up to invariant collision energy about 3.6 GeV.

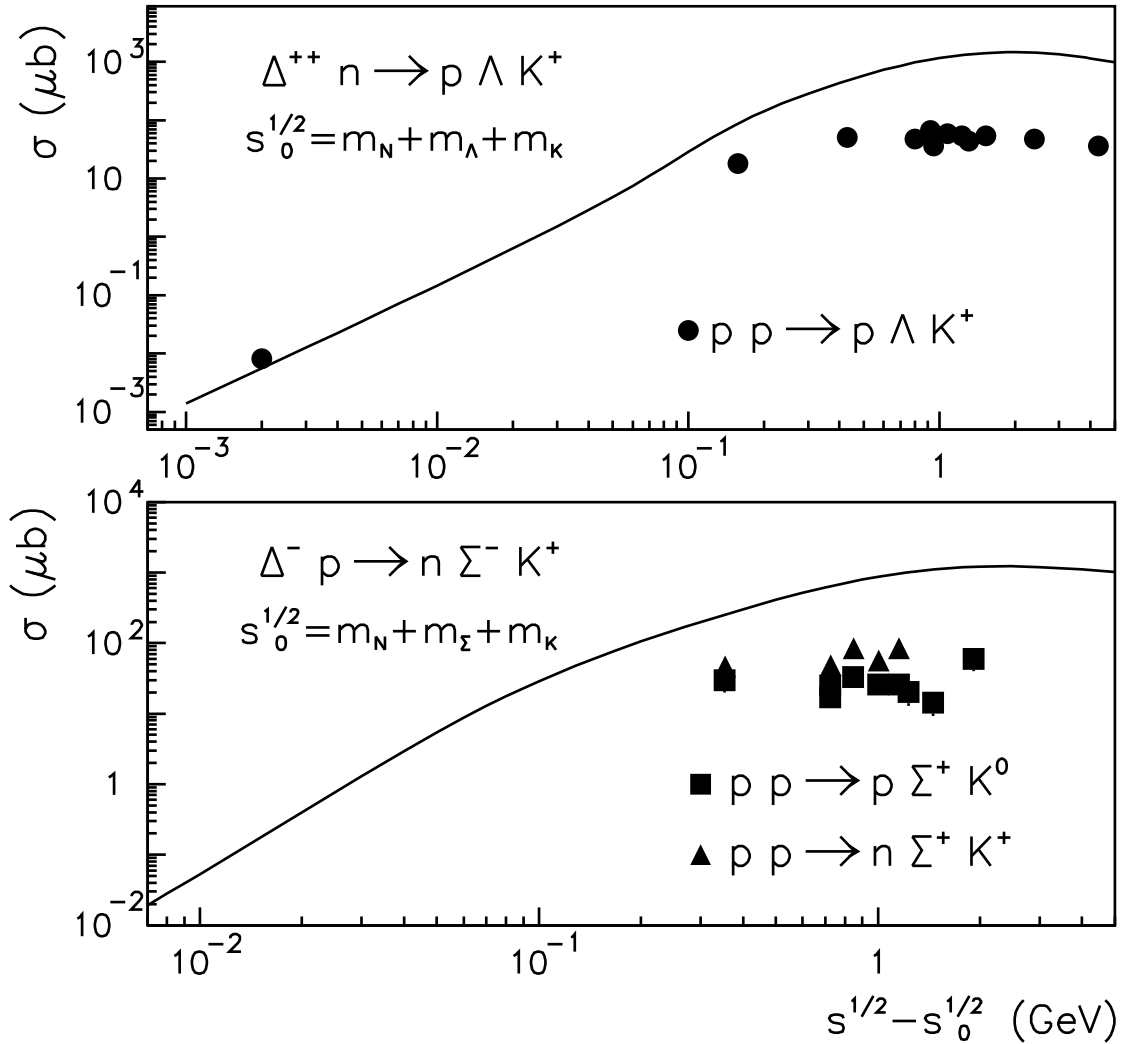
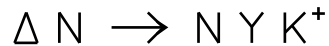


Figure 10: Energy dependence of the total cross sections for the $\Delta^{++}n \rightarrow p\Lambda K^+$ and $\Delta^-p \rightarrow n\Sigma^-K^+$ reactions. The dots, triangles and squares are the experimental data for the $pp \rightarrow p\Lambda K^+$, $pp \rightarrow p\Sigma^+K^0$ and $pp \rightarrow n\Sigma^+K^+$ reactions, respectively, from Ref. [49].

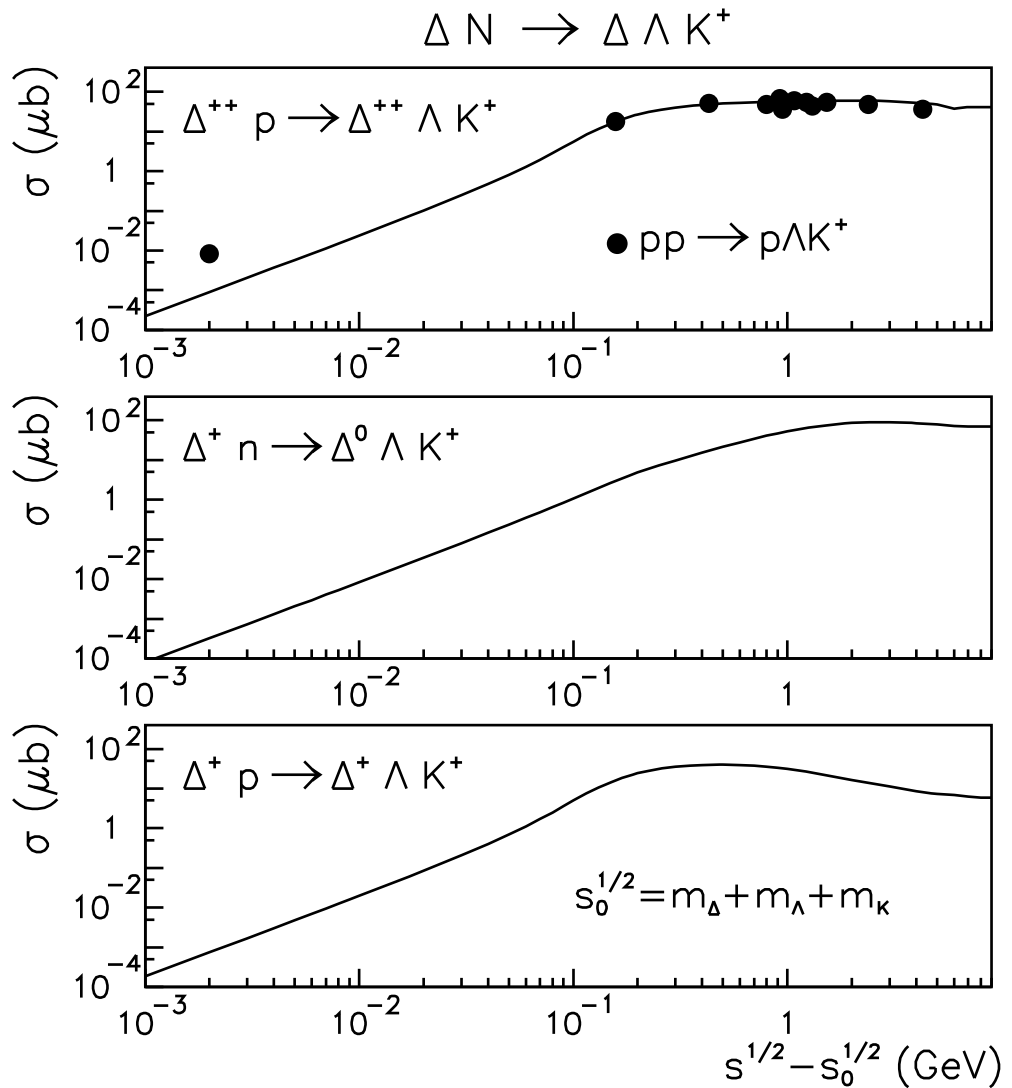


Figure 11: Energy dependence of the total cross sections for the $\Delta^{++}p \rightarrow \Delta^{++}\Lambda K^+$, $\Delta^+n \rightarrow \Delta^0\Lambda K^+$ and $\Delta^+p \rightarrow \Delta^+\Lambda K^+$ reactions. The dots are the experimental data from Ref. [49] plotted at the same excess energies from each threshold energy.

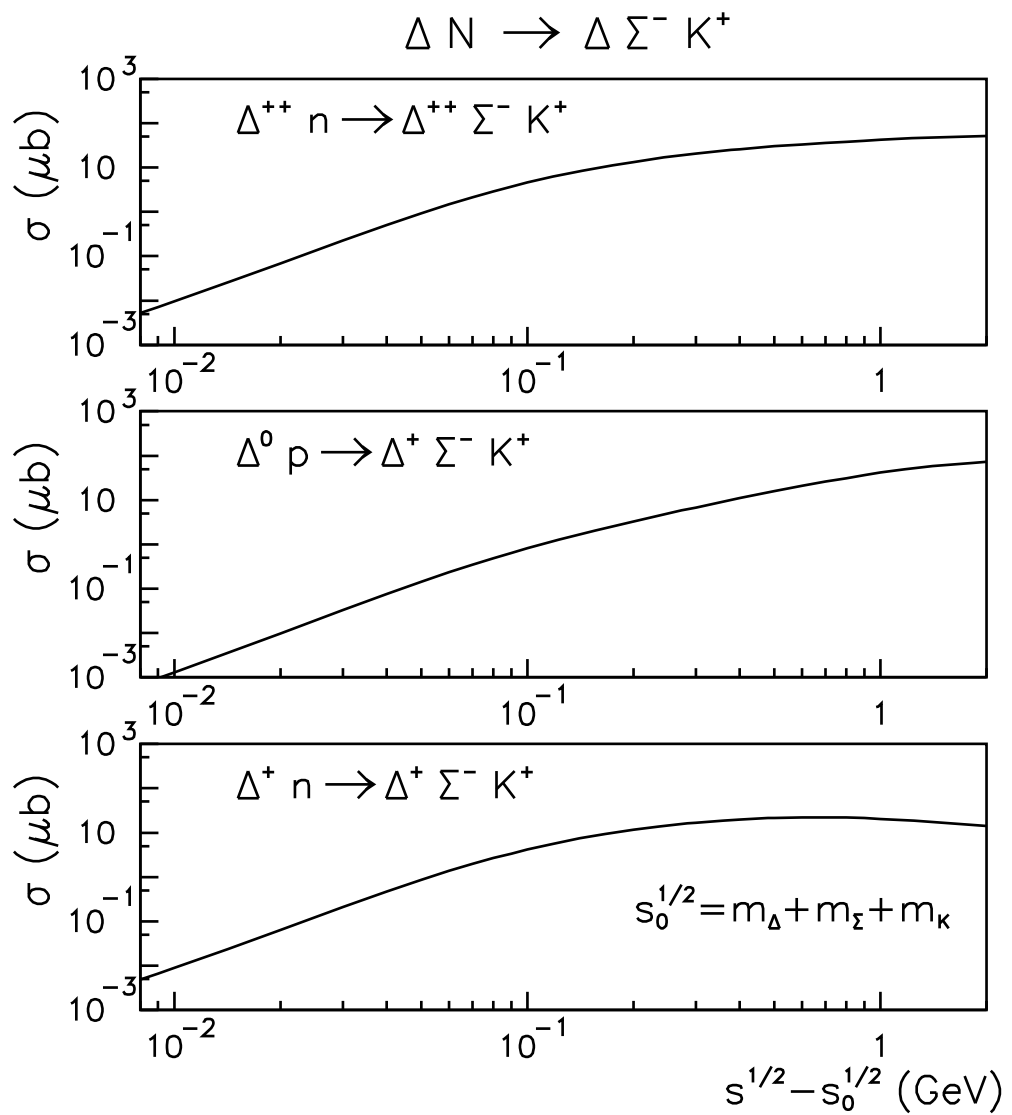


Figure 12: Energy dependence of the total cross sections for the $\Delta^{++}n \rightarrow \Delta^{++}\Sigma^-K^+$, $\Delta^0p \rightarrow \Delta^+\Sigma^-K^+$ and $\Delta^+n \rightarrow \Delta^+\Sigma^-K^+$ reactions.

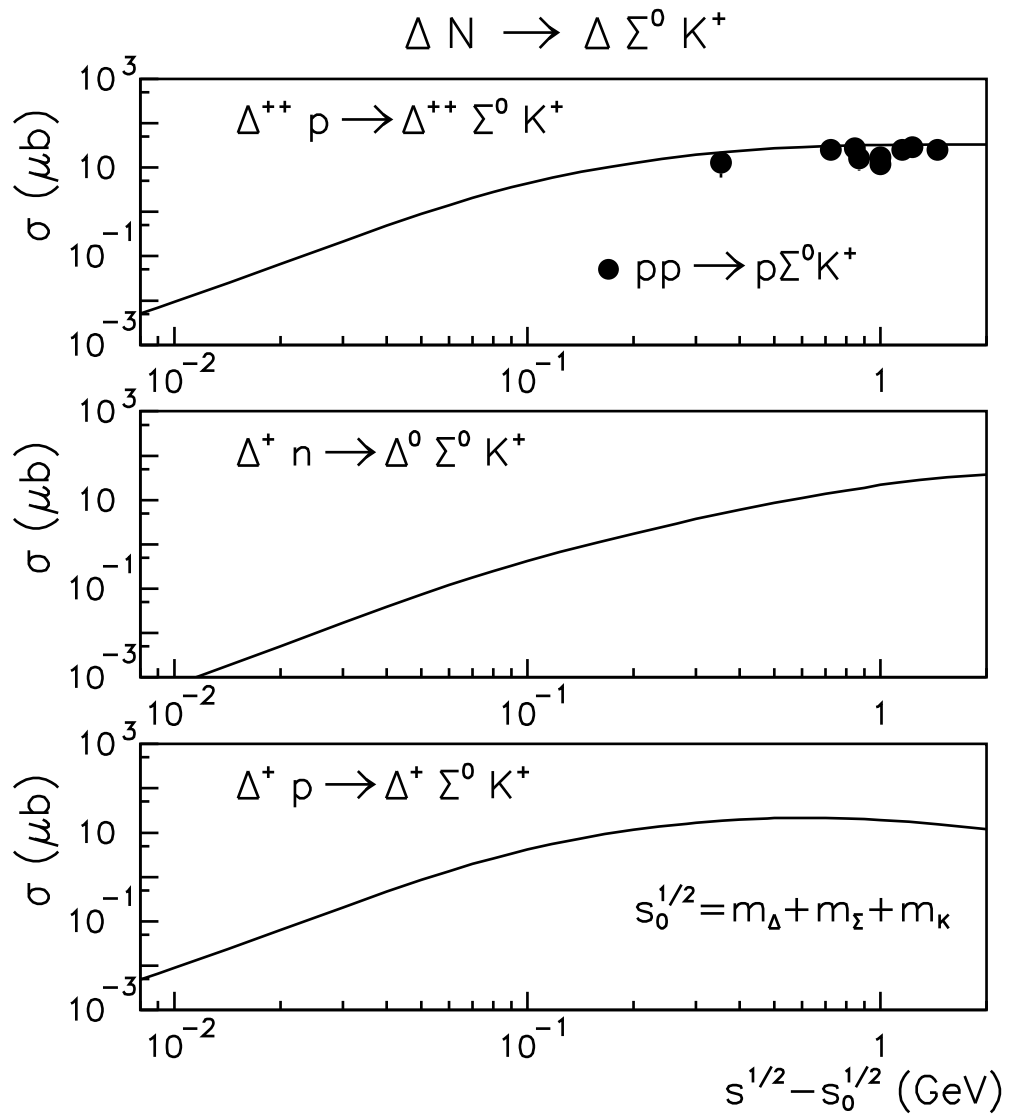


Figure 13: Same as in Fig. 11, but for the $\Delta^{++}p \rightarrow \Delta^{++}\Sigma^0K^+$, $\Delta^+n \rightarrow \Delta^0\Sigma^0K^+$ and $\Delta^+p \rightarrow \Delta^+\Sigma^0K^+$ reactions, and the data for the $pp \rightarrow p\Sigma^0K^+$ reaction.

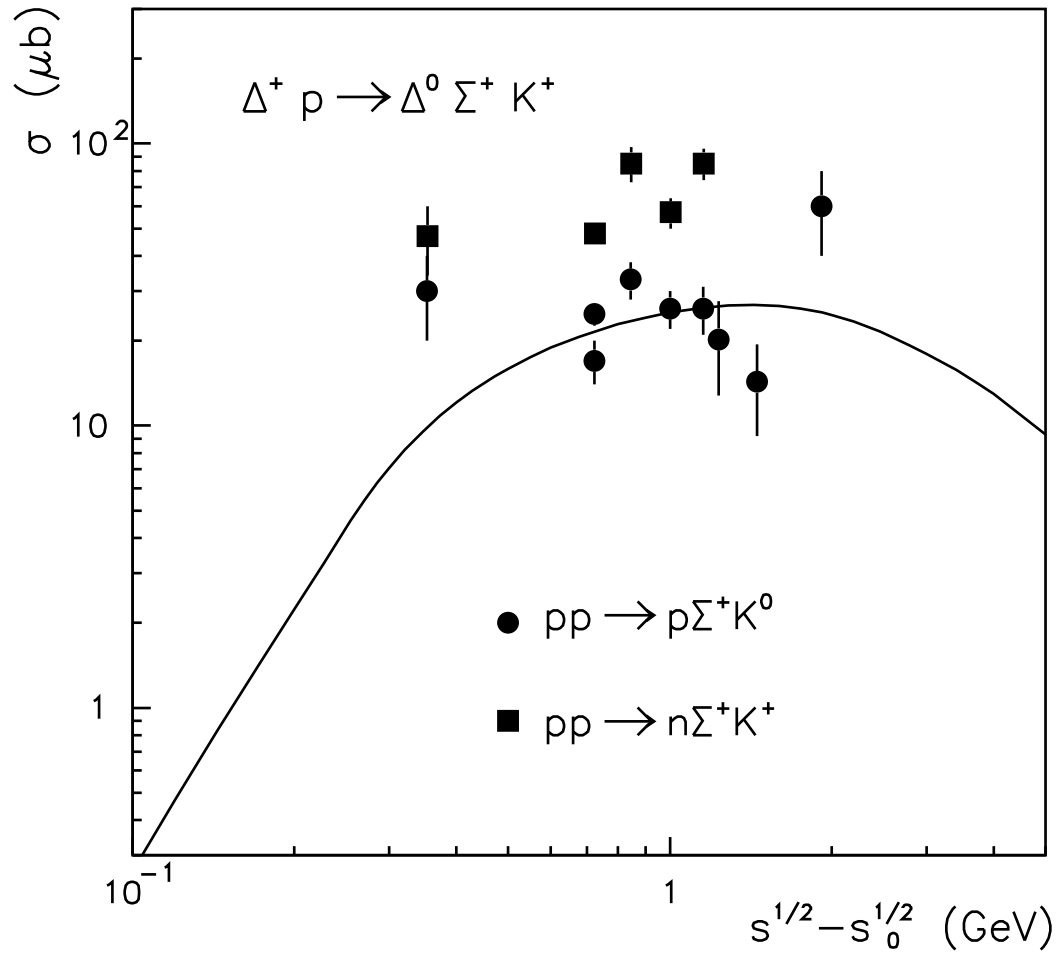


Figure 14: Energy dependence of the total cross sections for the $\Delta^+ p \rightarrow \Delta^0 \Sigma^+ K^+$ reaction together with the experimental data from Ref. [49] for the $pp \rightarrow p\Sigma^+ K^0$ and $pp \rightarrow n\Sigma^+ K^+$ reactions, plotted at the same excess energies. The threshold for the $\Delta^+ p \rightarrow \Delta^0 \Sigma^+ K^+$ reaction is $\sqrt{s_0} = m_\Delta + m_\Sigma + m_K$.

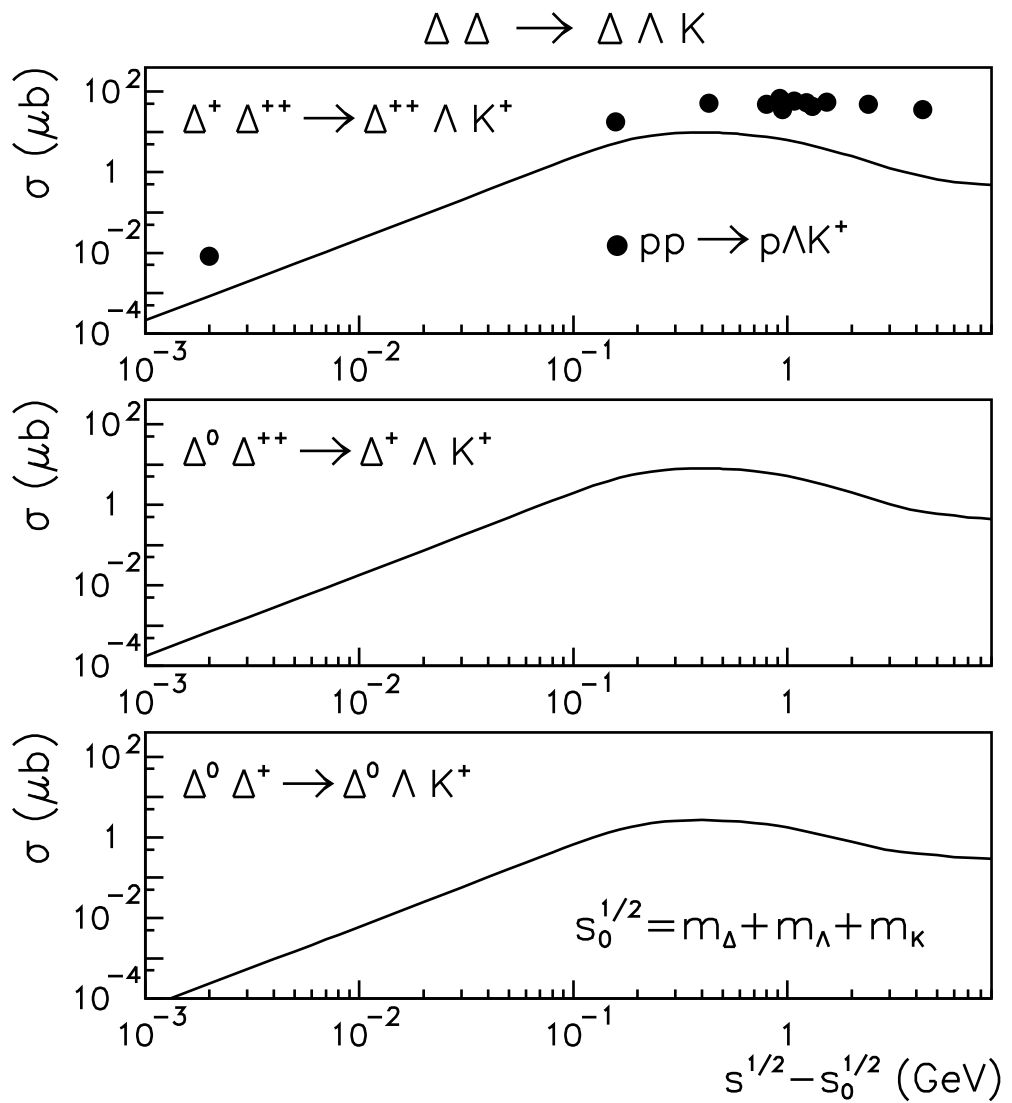


Figure 15: Same as in Fig. 11, but for the $\Delta^+ \Delta^{++} \rightarrow \Delta^{++} \Lambda K^+$, $\Delta^0 \Delta^{++} \rightarrow \Delta^+ \Lambda K^+$ and $\Delta^0 \Delta^+ \rightarrow \Delta^0 \Lambda K^+$ reactions.

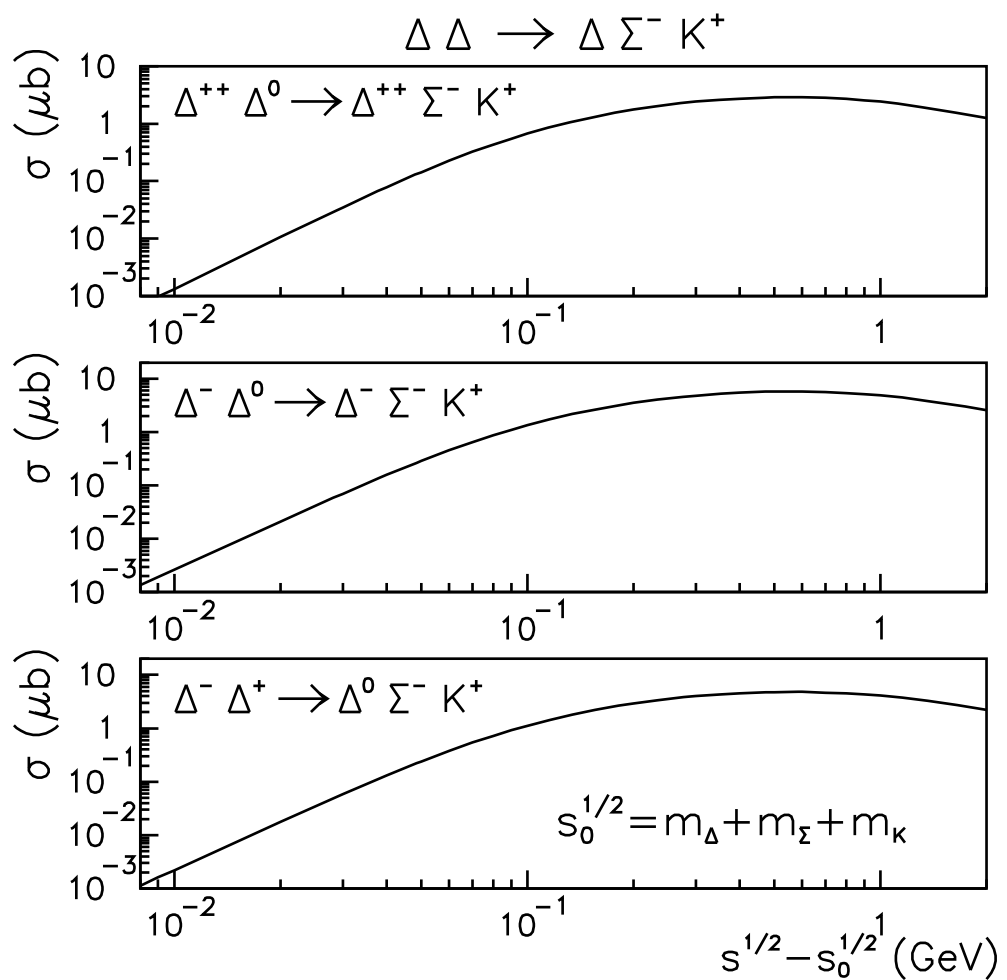


Figure 16: Energy dependence of the total cross sections for the $\Delta^{++}\Delta^0 \rightarrow \Delta^{++}\Sigma^- K^+$, $\Delta^-\Delta^0 \rightarrow \Delta^-\Sigma^- K^+$ and $\Delta^-\Delta^+ \rightarrow \Delta^0\Sigma^- K^+$ reactions.

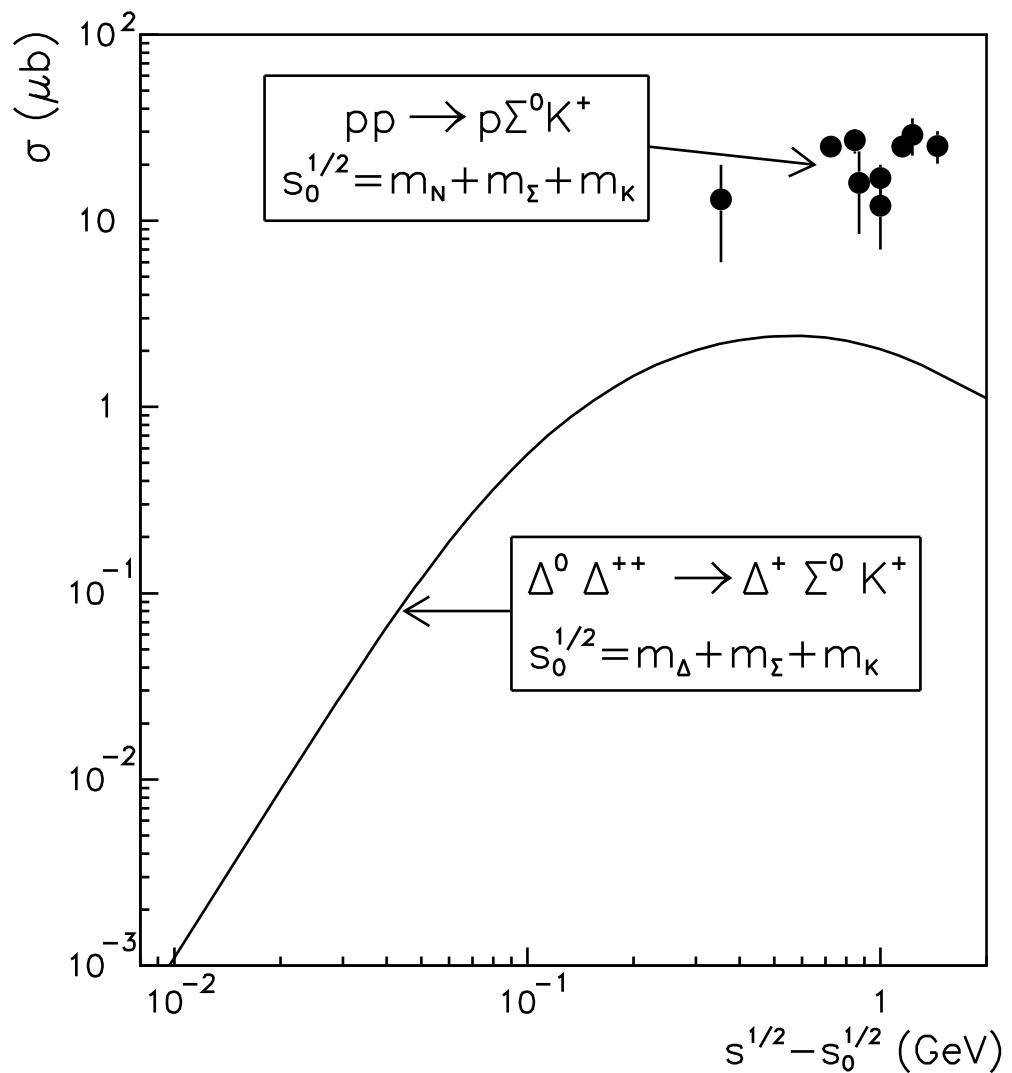


Figure 17: Same as in Fig. 14 but for the $\Delta^0 \Delta^{++} \rightarrow \Delta^+ \Sigma^0 K^+$ reaction and the experimental data are for the $pp \rightarrow p\Sigma^0 K^+$ reaction.

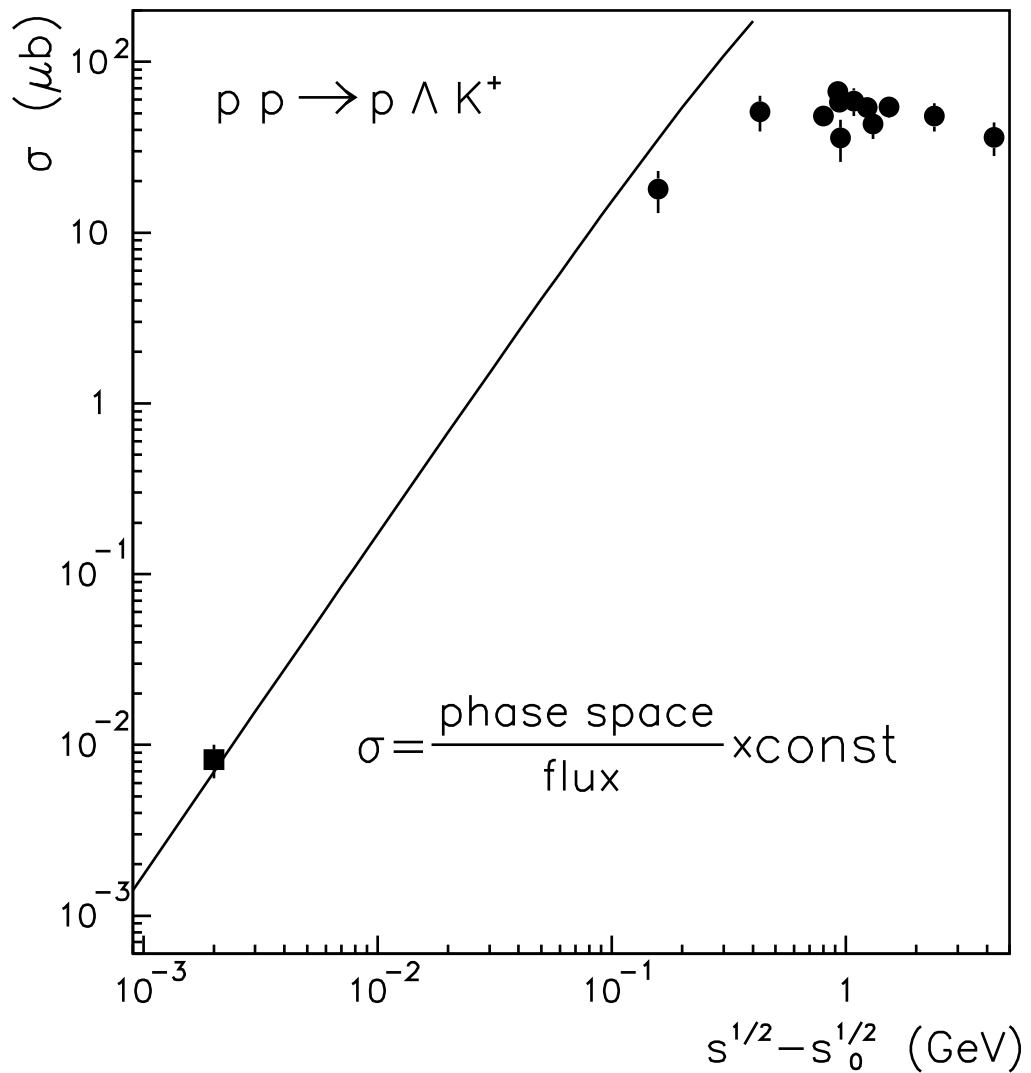


Figure 18: Phase space consideration of the total cross section for the $pp \rightarrow p\Lambda K^+$ reaction, according to Eq. (64). The dots and square show the experimental data from Ref. [49] and Ref. [34], respectively.

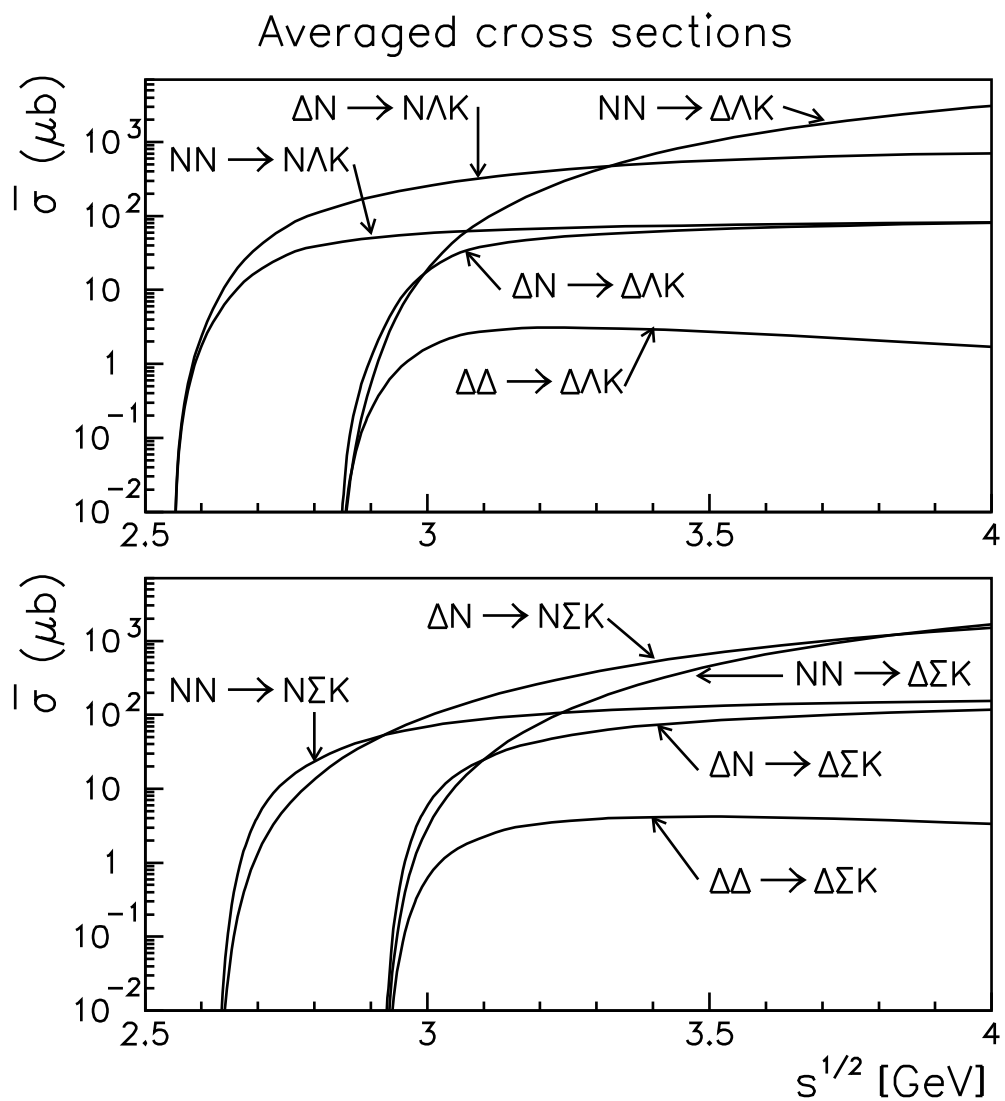


Figure 19: Energy dependence of the isospin-averaged total cross sections for the Λ and Σ production reactions in baryon baryon reactions.

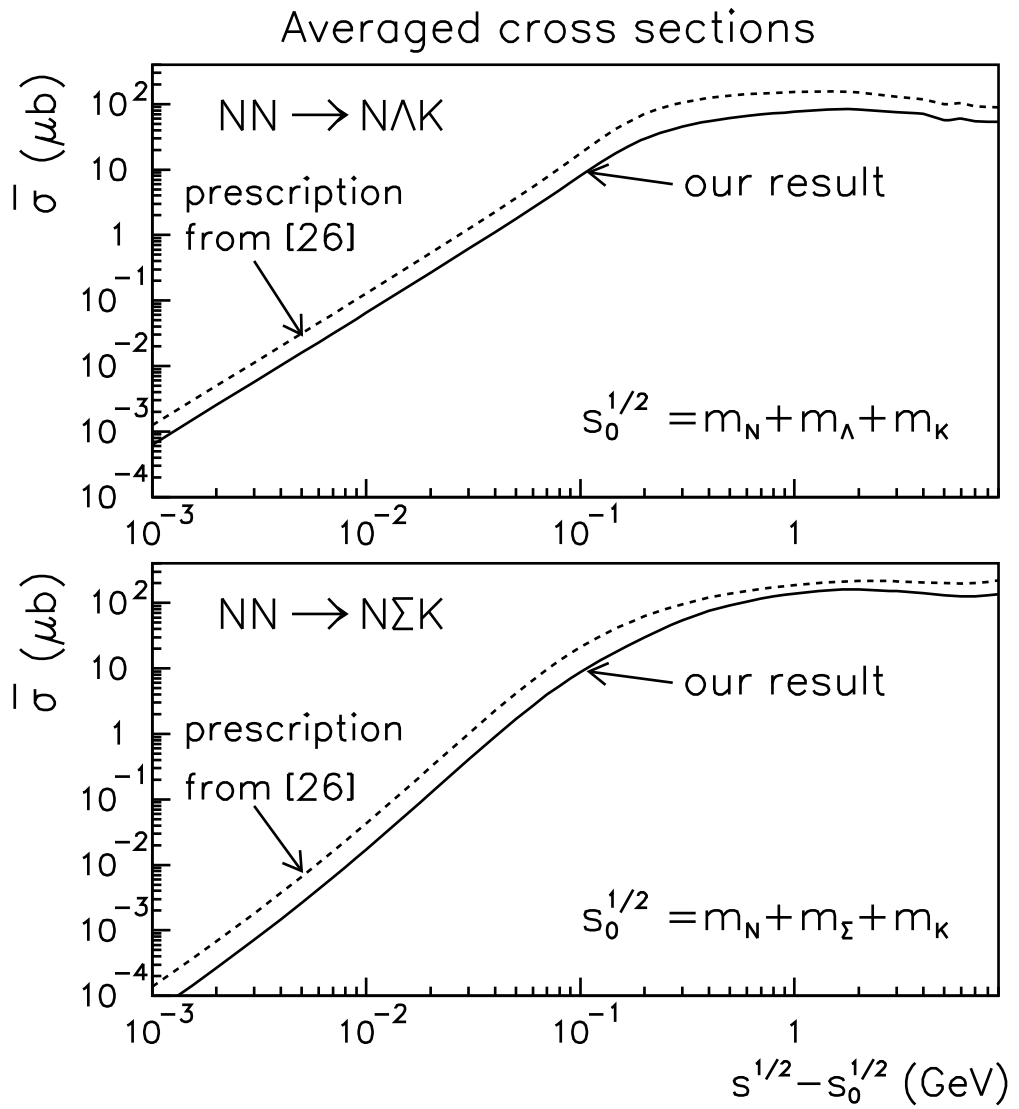


Figure 20: Energy dependence of the total cross sections both calculated in the model, isospin-averaged, and using the relations Eqs. (65) and (66) suggested by Randrup and Ko [26]. The solid lines show the model calculations for the isospin-averaged total cross sections (denoted by "our result"), while the dashed lines show the model calculations obtained using the right hand side of Eqs. (65) and (66) (denoted by "prescription from [26]").

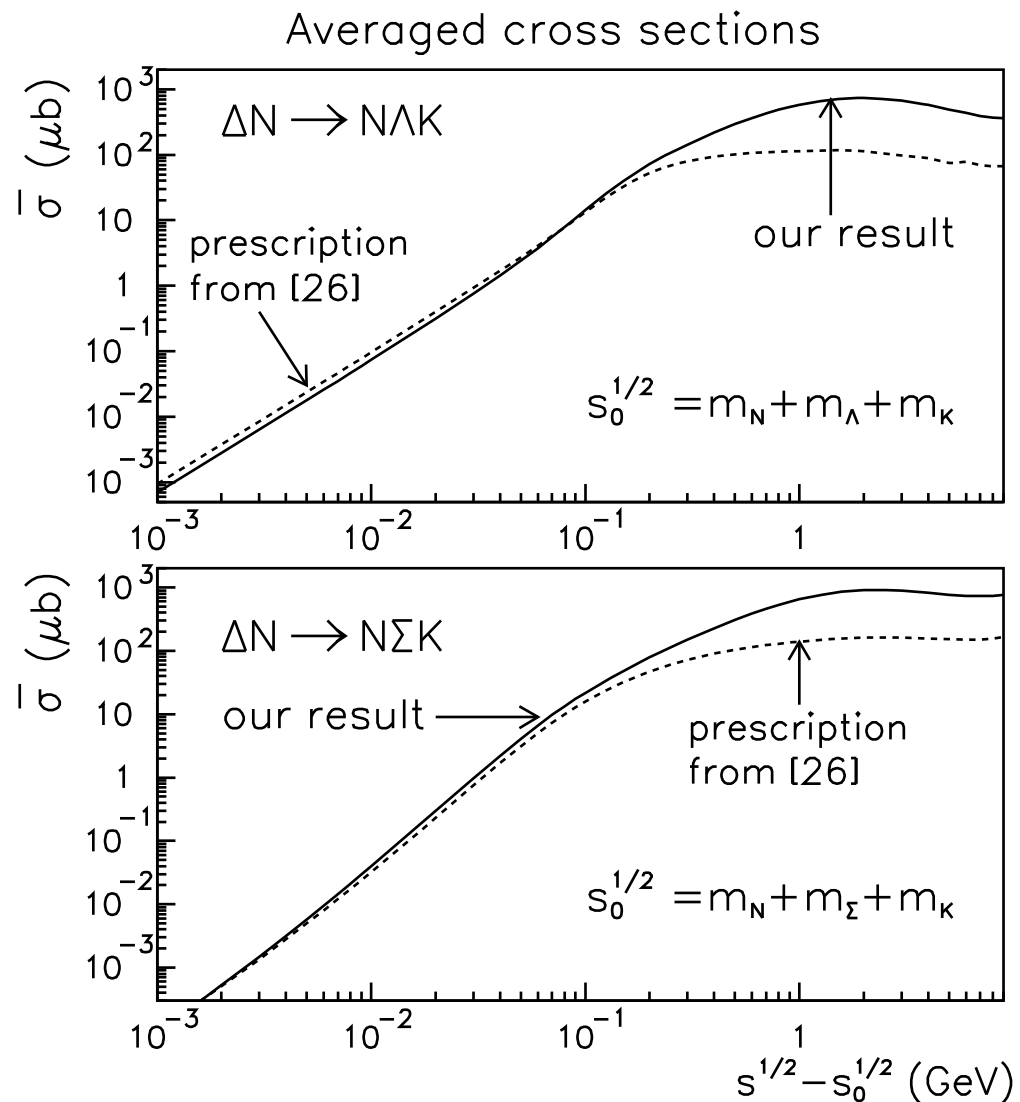


Figure 21: Same as in Fig. 20, but for the $\Delta N \rightarrow N\Lambda K$ and $\Delta N \rightarrow N\Sigma K$ reactions and Eqs. (67) and (68), respectively.

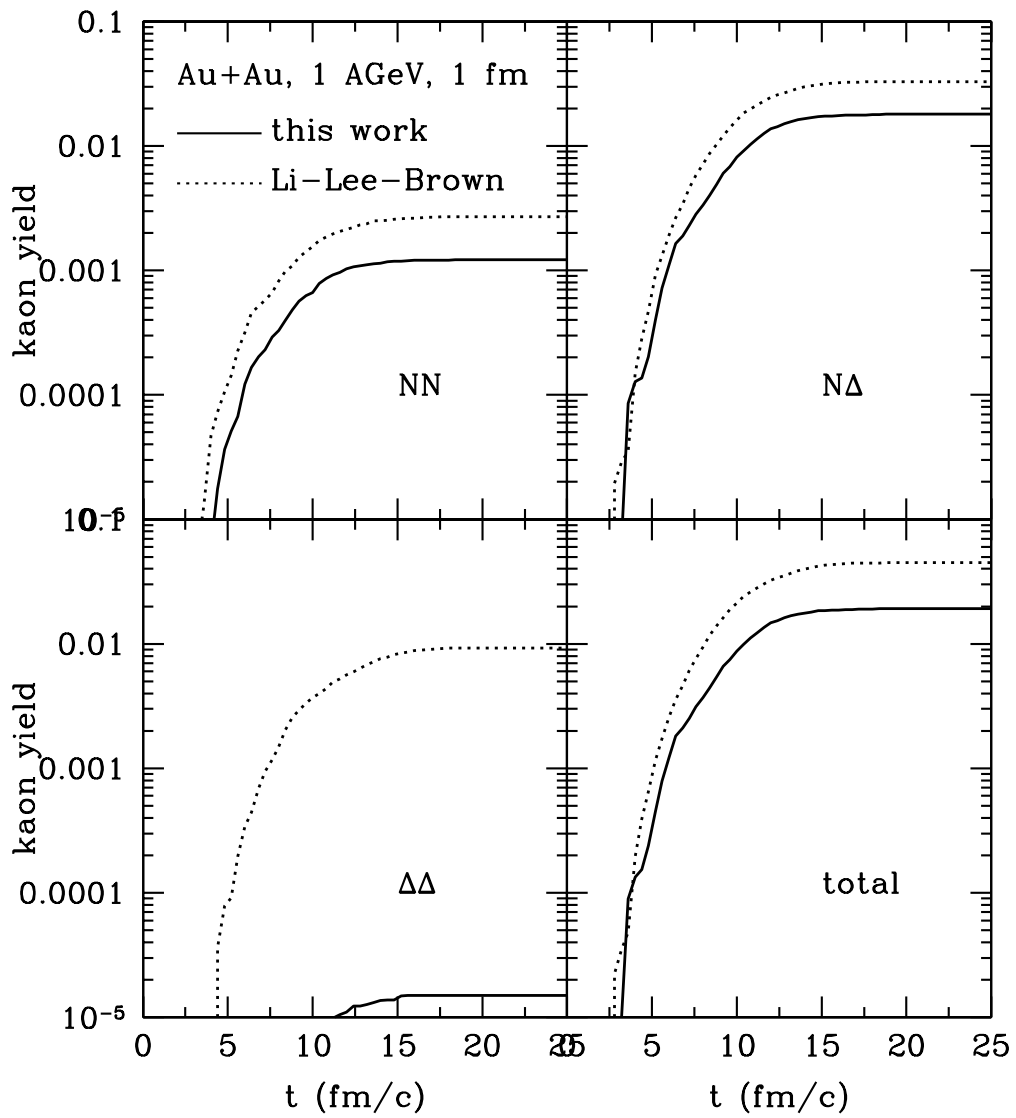


Figure 22: Kaon yield in Au+Au collisions at 1 AGeV and 1 fm obtained with two sets of elementary cross sections.

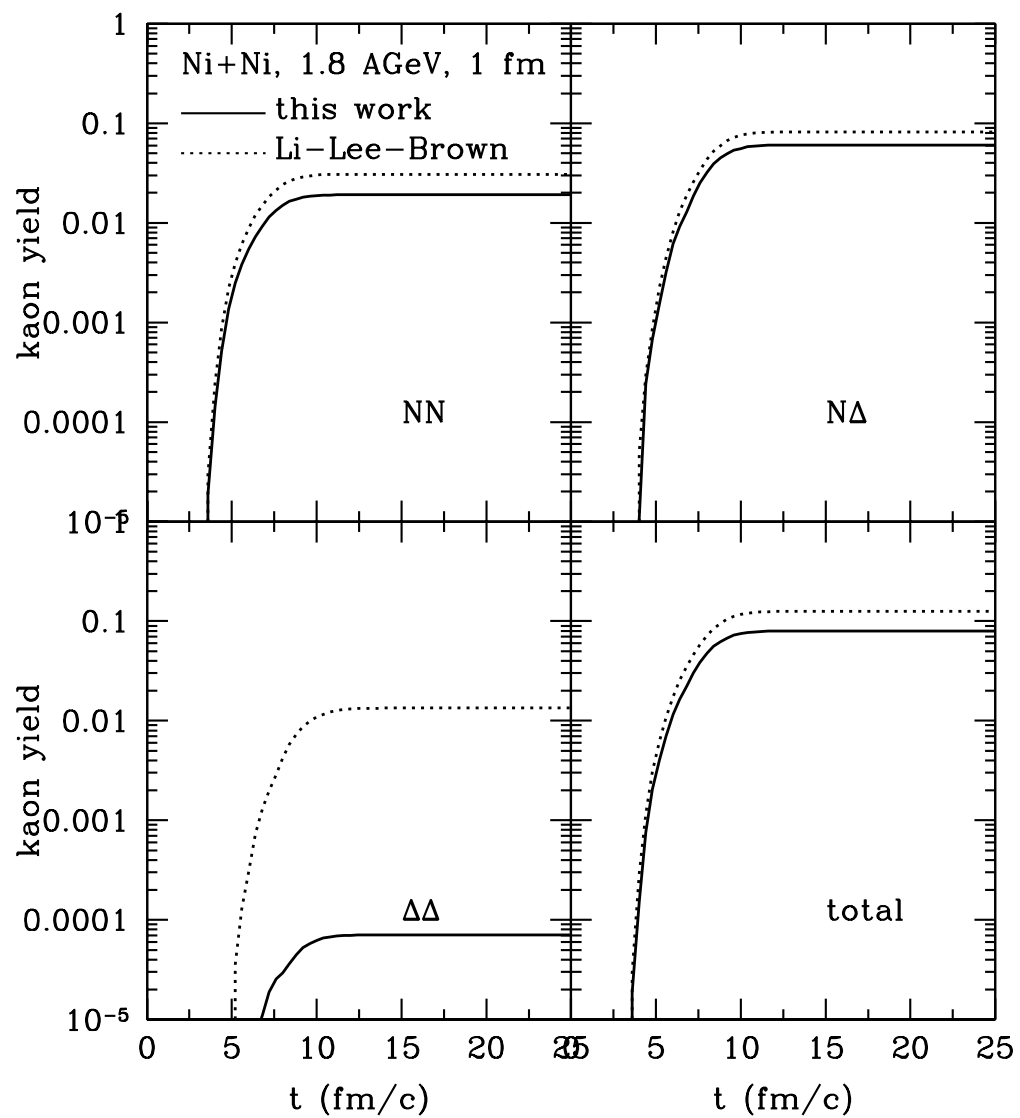


Figure 23: The same as Fig. 22, for Ni+Ni collisions at 1.8 AGeV.